Title
Characterization and Modification of Nanodiamond-Doxorubicin Complexes for Treatment of Colorectal Cancer

Author
Lee, Bryan

Publication Date
2015

Peer reviewed|Thesis/dissertation

UNIVERSITY OF CALIFORNIA

Los Angeles

Characterization and Modification of Nanodiamond-Doxorubicin Complexes for Treatment of Colorectal Cancer

A thesis submitted in partial satisfaction

of the requirements for the degree Master of Science

in Bioengineering

by

Bryan J. Lee

2015

ABSTRACT OF THE THESIS

Characterization and Modification of Nanodiamond-Doxorubicin Complexes for Treatment of Colorectal Cancer

by

Bryan J. Lee

Master of Science in Bioengineering

University of California, Los Angeles, 2015

Professor Dean Ho, Chair

Colorectal cancer is a leading cause of cancer death of the United States. Chemotherapy is a key component in the treatment of colorectal cancer. However, acquired resistance against chemotherapy and its inherent toxicity serve as major barriers to effective treatment. Nanodiamonds have been proven to overcome these barriers and can serve as a drug delivery platform for chemotherapeutics in human patients. The potential for this system needs to be explored further. In this thesis, a comprehensive study was performed on the production method of NDX (a complex of nanodiamond and doxorubicin) and its resulting physical characteristics. Ten batches of NDX were produced independently and the size and surface potential of the complexes were measured as well as their drug loading and drug release profiles. Analysis of the measurements displayed low standard deviation values across all the different parameters, illustrating a robust method for consistent production of NDX. Additionally, NDX could be

further functionalized for localized treatment of colorectal cancer. Thus, NDX-loaded liposomes (NDXLPs) were synthesized. These NDXLPs were stable in conditions designed to mimic the environment in the colon and also demonstrated an ability to penetrate a protective mucus layer. Therefore, this system represents a promising method to treat colorectal cancer. Futhermore, its flexibility for customization allows it to be utilized for a broader range of applications in cancer healthcare.

The thesis of Bryan J. Lee is approved.

Pei-Yu Chiou

Daniel T. Kamei

Dean Ho, Committee Chair

University of California, Los Angeles

2015

Dedication Page

I would like to thank Professor Dean Ho, Dr. Dong Keun Lee, and Kangyi Zhang for their guidance and mentorship throughout my time in the Master's program.

I would also like to thank the other professors on my thesis committee, Professor Daniel Kamei and Professor Eric Chiou for their time spent reviewing my thesis.

Table of Contents

Acknowledgements

Sections in this thesis are a version of:

"Characterization of the physical properties of nanodiamond-doxorubicin complexes"

Authors: Bryan Lee[1], Yusuke Fukuhara[2], Alan Grusky[3], James Huang[3], Kenneth Kim[3], Sam Noah[3], Dean Ho[*(corresponding author)]

This work is in preparation for submission to the Journal of Laboratory Automation (JALA).

The Nanodiamond-Doxorubicin (NDX) Synthesis section under Materials and Methods, the NDX Size and Zeta Potential Measurements, NDX Drug Loading Analysis, NDX Drug Release Analysis sections under Materials and Methods and Results, the first paragraph of the Discussion section and Tables 1-3 and Figures 1, 5 in this thesis are based on the above work.

Introduction

Colorectal cancer is the third most commonly diagnosed cancer and the second leading cause of cancer death in both men and women in the US. It is the most common form of gastrointestinal cancer. Over 136,000 people will be diagnosed in 2014 and over 50,000 will die from the disease in the US. The average lifetime risk of developing colorectal cancer is one in 20.[1] Patients with advanced metastasized colorectal cancer have a median overall survival of 9 months[2] and 5-year survival rate of 12%.[1] Surgical resection of the localized cancer leads to a very high curative rate if the cancer is discovered in the earlier stages before metastasis. However, the rate of recurrence reported in literature range anywhere from 13% to 61% for early stage colorectal cancers.[3] Significant survival benefit has been observed in patients who receive chemotherapy in addition to surgery versus surgery alone, in both adjuvant and neoadjuvant therapy. [2,4] Additionally, for patients with unresectable colorectal cancer, chemotherapy is the best treatment option. For example, first-line therapy for Stage IV colorectal cancer is a combination of different chemotherapeutic agents.

Unfortunately, the use of chemotherapy frequently leads to harmful side effects as well as the development of chemoresistance, rendering the drugs ineffective against the cancer cells. This acquired resistance contributes to treatment failure in over 90% of cases of metastatic cancer.[5] Studies have shown that p-glycoprotein, an essential protein in multidrug resistance, is highly expressed in colorectal cancers.[6–8] Patients receiving chemotherapy regimens for this disease can experience significant damage to the heart and liver among other organs. First line therapy chemotherapy regimens are often restricted in dosage by the accompanying toxic side effects.

Fortunately, nanodiamonds have emerged as a promising drug delivery platform to overcome chemoresistance as well as reduce chemo-induced toxicity. Nanodiamond-drug complexes have already been shown to be very effective in reducing multidrug resistant breast and liver tumors, in addition to glioblastoma, in rodent models without inducing the significant toxic side effects present in the models receiving only the drugs.[9–11] Thus, nanodiamond-enhanced chemotherapy can be a promising treatment option for late-stage colorectal cancer. Furthermore, they can be functionalized with liposomal carriers and targeting agents to enhance the specificity of delivery to metastasized cancer cells through systemic administration [9]. In addition, the nanodiamond-liposome particles can be used for localized treatment of early stage colorectal cancer as part of adjuvant therapy. Localized delivery of chemotherapeutics with nanodiamond-liposome particles would provide a more effective and safer alternative to standard chemotherapy.

Doxorubicin for treatment of cancer and its associated side-effects

Doxorubicin (Dox) is a chemotherapeutic drug and is categorized as an anthracycline, a specific class of drugs derived from Streptomyces bacterium. Doxorubicin as well as other anthracyclines function by intercalating DNA. Dox binds to DNA and inhibits the enzyme topoisomerase II from resealing the double helix structure, thus stopping the replication process. Dox is used to treat a wide range of cancers including breast, ovarian, stomach, and certain types of leukemia.[12] Anthracyclines and Dox, in particular, can cause significant myelosupression and cardiotoxicity, severely limiting the dosage that can be used in chemotherapy regimens.[12] Dox also contributes to significant tissue damage in the liver and kidneys, with 40% of patients

undergoing treatment experiencing some form of liver injury[12] and as much as 40% experiencing grade 3 or 4 neutropenia[4].

Resistance to chemotherapy treatment

Multidrug resistance is a mechanism in which many cancers can develop resistance to chemotherapeutic agents. It exists in a broad range of cancers including breast, ovarian, lung, and lower gastrointestinal tract cancers.[13] Multidrug resistance is largely responsible for many cases of recurrent cancers since the resistant population escapes apoptosis and eventually grows again. Now the recurrent cancer is predominantly resistant to chemotherapy, requiring a completely new regimen. This leads to the use of second-line and potentially third-line therapy regimens. Needless to say, multidrug resistance presents a major roadblock to successful chemotherapy treatment.

Multidrug resistance is mainly attributed to ATP-binding cassette (ABC) transporters, proteins within the cell membrane that function as molecular 'pumps'. Two ABC transporters in particular, MDR1(also called P-glycoprotein) and MRP1, are expressed in many human cancers.[13] These proteins actively transport substrates such as chemotherapeutics from the cytoplasm to the exterior of the cell. This action is known as efflux. Since many chemotherapeutics such as Dox need to enter the nucleus in order to induce their cytotoxic mechanisms, effluxing the drugs out of the cell renders them ineffective.

Because these ABC transporter proteins are essential in conferring chemoresistance, chemical inhibitors against MDR1 and MRP1 have been explored. These chemical inhibitors are

used to sensitize the cancer cells to chemotherapy. Researchers have performed many studies using various chemical inhibitors in combination with Dox for treatment of colorectal cancers. Inhibitors such as verapamil and fluoxetine have been shown to successfully reverse drug efflux of Dox in human colorectal cancer cell lines.[14,15] Some other inhibitors are much more specific: amooranin competitively inhibits MDR1-mediated Dox efflux[16] while Fumitremorgin C overcomes resistance in colorectal cancer cell lines with non-MDR1 and non-MRP associated multidrug resistance.[17] On the other hand, there are inhibitors—tamoxifen and dexverapamil—that did not improve therapeutic effect of Dox in this disease model in the clinical setting.[18] Overall, chemical inhibitors of ABC proteins vary in efficacy, due to the variation in drug transporters that mediate chemoresistance, as well as toxicity.[19,20] Therefore, a passive mechanism to overcome multidrug resistance would potentially be more effective.

Nanodiamonds enhance therapeutic efficacy of Doxorubicin

Nanodiamonds are carbon nanoparticles with a diamond shaped structure. The core of nanodiamonds are made up of purely sp^3 carbons while the surface must be stabilized with functional groups or conversion into sp^2 carbons. Thus, processed nanodiamond surfaces have a rich amount of carboxylic acid functional groups. This provides abundant options for surface functionalization, allowing nanodiamonds to be customized for a broad range of applications.[21] Furthermore, nanodiamonds have demonstrated good biocompatibility. Previous studies show that nanodiamonds do not induce cellular apoptosis as well as cellular inflammation.[22] Also, nanodiamonds administered at high dosages did not change the levels of serum indicators of liver and systemic toxicity.[21] Nanodiamonds have proven to be an effective drug delivery platform for

various therapeutic molecules including Cytochrome c[23], plasmids[24], siRNA[25], and anthracyclines.[9–11]

Synthesis of nanodiamond-doxorubicin complexes (NDX) is quick, simple, and scalable. It utilizes sodium hydroxide to trigger strong electrostatic interaction between the nanodiamonds and the Dox molecules. A potential mechanism for the formation of NDX is the attraction between protonated amines on the Dox molecules and deprotonated carboxylic acid groups on the surface of the nanodiamonds. This electrostatic binding between Dox and the nanodiamonds is reversible. Previous studies have demonstrated that Dox released from nanodiamonds is still fully functional.[11]

In particular, studies have shown NDX to be very effective in the treatment of drug resistant breast and liver cancers. NDX has a much longer circulation half-life (8.43 hr) versus free Dox (0.83 hr).[11] This increased systemic circulation time enhances accumulation of the complexes in the tumor sites due to the EPR effect. Once endocytosed, NDX is difficult to be ejected out of the cell by the drug transporters due to the size of the complexes. NDX exhibits a sustained release of Dox rather than an immediate release of all drug cargo. This mechanism impairs Dox efflux by the ABC transporter proteins and significantly enhances Dox retention within the tumor tissue, thus maintaining a high intracellular concentration of the drug. Previous studies demonstrate that the efficacy of NDX is unaffected by verapamil, a universal drug transporter inhibitor, suggesting that NDX bypasses the efflux mechanism.[11] Therefore, NDX mediates a prolonged exposure to a high concentration of Dox within the cancer cells, which results in increased cell death. NDX's ability to overcome efflux-based chemoresistance is more

advantageous versus that of chemical inhibitors because of its lack of dependence on specificity for different transporters.

Additionally, NDX improves drug tolerance by reducing chemo-induced toxicity. The strong interaction between nanodiamond and Dox within the complexes reduces exposure of the drug in systemic circulation. NDX almost eliminates Dox-associated myelosuppression, a dose-limiting side effect.[11] Furthermore, an extremely high dosage of free Dox (200 μg) that resulted in mortality in one model, did not result in mortality while incorporated with nanodiamond.[11] In fact, NDX with 200 μg of Dox further increased tumor apoptosis.

Characterization of the physical properties of NDX

NDX represents a promising drug delivery platform for enhancing chemotherapy in drug resistant cancers and reducing chemo-induced toxicity. However, there remains extensive translational work to be done to determine the efficacy of NDX in human patients. As a part of this process from the benchtop to clinic, a comprehensive study of the physical characteristics of NDX must first be performed. Among the properties that need to be considered for nano-scale drug carriers are particle size, surface charge, drug loading and drug release. Multiple batches of NDX will be analyzed in order to demonstrate a robust and consistent method for the production of NDX.

Functionalization of NDX for localized delivery to colorectal cancers

Moore et al. have previously demonstrated functionalization of nanodiamond-epirubicin complexes (NDE) for targeted delivery of chemotherapeutics. This study encapsulated NDE in

liposomal carriers and covalently attached anti-EGFR antibodies to the surface of the carriers. These resulting nanodiamond-lipid hybrid particles (NDLPs) were injected systemically into rodent models to treat breast cancer xenografts. The experimental results from this study demonstrate improved drug tolerance and even tumor regression compared to NDX, due to improved selectivity of cancer cells through its active targeting mechanism.[9] Thus, NDLPs have potential as an effective treatment option for patients with metastasized cancers.

Furthermore, incorporation of nanodiamond-drug complexes in liposomes can be utilized for an alternative application—localized delivery. As previously mentioned, the most successful method to cure colorectal cancers discovered in the earlier stages involves a combination of surgical resection to remove the tumor mass and accompanying chemotherapy to eliminate remaining cancer cells. The chemotherapy regimen is typically administered systemically, resulting in a multitude of adverse side effects. Additionally, there is a significant cancer recurrence rate likely due to the presence of cancer cells that developed chemoresistance. Therefore, a drug delivery platform such as NDX that can overcome chemoresistance mechanisms should be used in order to effectively kill off resistant cells and prevent cancer recurrence. However even with NDX, minor toxicity was still present since there is still exposure to the drug in areas of the body due to systemic distribution. Administering NDX locally to the tumor site area in the colon would avoid any toxicity to other areas. This could be done post-surgery by implanting a degradable, biocompatible device such as a hydrogel in a section of the colon near the tumor site that would gradually release NDX for localized treatment. Another way to administer NDX locally would be through a barium enema in a degradable gel.

Still, local delivery of particles in the colon does present certain challenges. Among those challenges are a highly ionic environment and a protective mucus layer. Nanodiamonds tend to aggregate in ionic environments due to ionic shielding eliminating electrostatic repulsion between the diamond particles.[9] The mucus barrier is essentially a viscoeleastic gel composed of 95% water and 1.0 to 5% heavily glycosylated high molecular weight proteins known as mucins.[26] The mucus layer is a key defensive mechanism within the gastrointestinal tract that traps foreign particles, preventing their exposure to tissues and organs in the body. Mucins form a mesh network that block larger particles from diffusing through. They also feature extensive negatively charged sugar moieties. With its highly positive surface charge, NDX would certainly be strongly attracted to mucins. Additionally, NDX would experience severe aggregation because of the ionic environment. Thus, the mucus barrier would trap a vast majority of the NDX preventing them from ever reaching the underlying epithelium in the colon where the cancer cells reside, thus severely limiting treatment efficacy.

NDX must be modified in order to be an effective system for localized delivery in the colon. Size aggregation must be prevented to allow complexes to fit in the pores of the mucin mesh network. Also, the surface charge of the complexes must be reduced to prevent adhesion to the negatively charged mucins. Incorporation of NDX with a liposomal carrier presents a solution to resolve these issues. Liposomes composed of phosphatidylcholine have slightly negative surface potentials.[27–29] When the surfaces of these liposomes are outfitted with nonionic long chain polymers such as polyethylene glycol (PEG) or Pluronics (tri-block copolymers), the negative charge is further reduced and the zeta potential is very close to zero.[9,27–32] In addition, long chain polymers reduce aggregation of liposomal particles as well as accelerate their diffusion through mucus barriers due to steric effects.[27–29] These particles are also stable in high

ionic environments.[9,28] Therefore, encapsulation of NDX within liposomal carriers equipped with long polymer chains combines the abilities to overcome chemo-resistance, minimize drug toxicity, and penetrate the protective mucus barrier lining the colorectal epithelium. In this study, NDX-loaded liposomes (NDXLPs) will be synthesized, characterized, and tested for their stability in high ionic environment of varying pH as well as their mucus penetrating ability.

Materials and Methods

Nanodiamond-Doxorubicin (NDX) Synthesis

Nanodiamonds were provided by NanoCarbon Research Institute Ltd. (Matsumoto, Nagano, Japan). The nanodiamonds were dispersed in water at a concentration of 5mg/mL. Sonication was performed with a probe sonicator (Model FB-705, Fisher Scientific, Pittsburgh, PA) prior to synthesis using the following settings: Amplitude 40, Process Time 5 min, 40 sec pulse on, 10 sec pulse off. A solution of aqueous doxorubicin (Doxorubicin-HCl, Sigma-Aldrich, St. Louis, MO) was prepared at a concentration of 10 mg/mL. The nanodiamonds were then mixed in solution with doxorubicin (Dox) at a ratio of 5 mg of nanodiamonds to 1 mg of Dox. The pH of the solution is adjusted to 7.74 with a final concentration of 2.5 mM NaOH to facilitate drug loading. The mixture was then stored away from light at room temperature and allowed to incubate for 24 hours. After incubation, the mixture was centrifuged at 3,000xg for 15 min. The supernatant was removed and kept for spectroscopic analysis. The NDX pellet was then redispersed in water with the probe sonicator. The sample was then centrifuged at 3,000xg for 15 min a second time and the supernatant was again removed and kept for analysis. Finally, the NDX pellet was redispersed in water at a concentration of 5 mg/mL of ND with the probe sonicator.

NDX Size and Zeta Potential Measurements

The z-average size, size distribution, and zeta potential of the NDX particles were measured using Malvern Zetasizer Nano-ZS from Malvern Instruments (London, UK). The measurements

were performed at 25°C at a scattering angle of 173°. Measurements were performed in triplicate.

NDX Drug Loading Analysis

Spectroscopic analysis was performed using a microplate reader. The absorbances of both supernatant samples were measured at a wavelength of 550 nm. The absorbance values of the supernatant samples were then compared against a standard curve (obtained by serial dilution of Dox in 2.5 mM NaOH) to determine their concentrations. Based on the concentration of Dox in the supernatant and the volume of the supernatant, the total amount of Dox in the supernatant was determined. The loading efficiency was calculated with the following formula: **Loading efficiency** = (Initial amount of Dox added – Total amount of Dox in Supernatant)/ Total amount of Dox in Supernatant x 100%

NDX Drug Release Analysis

NDX samples were diluted to an initial concentration of 0.1 mg/mL in terms of Dox. The samples were then centrifuged at 18,000xg for 30 min. 100 μL of the supernatant was extracted and measured for absorbance to determine the amount of Dox released initially in water. The supernatant was then discarded and the NDX pellet in those samples was resuspended in media [composed of 10% fetal bovine serum(Gemini Bio-products, Sacramento, CA) in Dulbecco's Modified Eagle Medium (DMEM) (Life Technologies, Carlsbad, CA)] diluted 1:1 and 1:10 in PBS and then incubated at 37°C. After incubation, the samples were centrifuged at 18,000xg for

10 min. 100 μL of the supernatant was extracted for Dox fluorescence measurement (excitation: 480 nm; emission: 550 nm) on hr 1, 2, 3, 4, 5 on day 1 and everyday until day 10. The experimental samples for fluorescence measurement were performed in triplicate. After measurement, the supernatant is discarded, and the NDX pellet is resuspended with fresh media and incubated as explained previously. The fluorescence values for the supernatant are then compared against the corresponding standard curve (obtained by serial dilution of Dox in 1:1 media or 1:10 media) to determine their concentrations and consequently the total amount of Dox after factoring in the volume of the supernatant. For every time point, the cumulative amount of Dox released up to that point is taken into account. The percentage of Dox released is based on the amount of Dox initially adsorbed onto the NDs.

NDX-Loaded Liposomes (NDXLPs) Synthesis

NDXLPs were synthesized by hydration of lipid thin films with concentrated NDX solutions. Egg phosphatidycholine (EPC), cholesterol (Chol), and Pluronic F-127 (PF-127) were mixed in chloroform in a molar ratio of 100:10:3 EPC: Chol: PF-127 and added to a round-bottom flask. For fluorescent analysis purposes, 1,1'-dioctadecyl-3,3,3',3'-tetramethylindodicarbocyanine perchlorate (DID), a lipid-soluble dye, was added to the lipid mixture at a concentration of 1% wt. The chloroform is removed using a rotary evaporator leaving a lipid thin film in the flask. The lipid film is rehydrated with NDX (5mg/mL in water) with 4:1 ratio of EPC: ND by weight. A bath sonicator is used to break down particles adhered to the flask. The solution is transferred from the round-bottom flask into a separate tube. The NDXLPs are then sized with a probe sonicator (Amplitude 40, Process Time 1 min, 15 sec pulse on, 30 sec pulse off) while in a cold

water bath. The solution is then diluted into PBS and filtered with a mini-extruder (Avanti Polar Lipids, Alabaster, AL) and a 0.2μm polycarbonate membrane (Whatman, Pittsburgh, PA)

NDXLP Size and Zeta Potential Measurement and Fluorescence Analysis

The z-average size, size distribution, and zeta potential of the NDXLP particles were measured using the Zetasizer. The measurements were performed at 25°C at a scattering angle of 173°. Measurements were performed in triplicate. Fluorescence measurements were also taken for the NDXLPs using a spectral scanning option on a microplate reader.

NDXLP Size Exclusion Chromatography Analysis

Size exclusion chromatography (SEC) was performed using Sepharose CL-4B resin (Sigma-Aldrich). The resin was packed to a final column volume of 10 mL. The column is equilibrated with PBS. The NDXLP solution is loaded onto the column and separated into approximately 1 mL fractions. The fractions are then analyzed for the fluorescence signals of NDX (excitation 480 nm; emission 590 nm) and DID (excitation 600 nm; emission 670 nm) using a microplate reader.

Thermo-stability of NDXLP

NDXLPs are incubated at 37°C in PBS. Size measurements are taken using the Zetasizer after 1, 2, 3, and 4 hours of incubation.

NDXLP zeta across pH range

The pH of the NDXLP solution in different samples is adjusted to the following values: 5.6, 6.0, 6.4, 6.8, 7.2, and 7.6. Zeta potential measurements for the NDXLPs across the pH range are taken using the Zetasizer.

Mucus Penetration Studies

Mucus penetration studies were performed using a Transwell plate with 3.0 μm polyester membranes with a surface area is 0.33 cm^2 (Corning, Corning, NY). One set of membranes was coated with 2% wt porcine mucin (Sigma-Aldrich) and another set was coated with 5% wt mucin such that the thickness of the mucus layer is 150 μm. One set of membranes was left uncoated and serves as the control. The bottom compartments are filled with 600 μL of PBS, while the top compartments were filled with 100 μL of NDXLP solution with a concentration of 2 mg/mL lipid. The particles were allowed to diffuse through the membrane and mucus layers for 2 hrs and 4 hrs. The solution from the bottom compartment was extracted after those timepoints and analyzed for DID fluorescence (excitation 600 nm; emission 670 nm) with a microplate reader. The fluorescent values for the solution in the bottom compartment were then compared against a standard curve obtained by serial dilution of the NDXLP solution at specified concentrations. The total amounts of NDXLPs that passed into the bottom compartment for each group (control, 2% mucin, 5% mucin) were then determined. The amount of NDXLPs that passed through the mucus layers were then divided by the amount from the control and multiplied by 100% for each time point to achieve values for percentage penetration.

Results

NDX Size and Zeta Potential Measurements

After NDX synthesis for each batch, dynamic light scattering (DLS) was performed to determine the z-average size of the complexes. Zeta potential measurements were also performed. Refer to **Table 1** for the values for all 10 batches of NDX. The NDX complexes had an average size of 116.7 ± 6.4 nm. The particles also exhibited a narrow size distribution with an average polydispersity index (PDI) of 0.18. The average zeta potential of the particles was +50.3 ± 3.1 mV. Statistical analysis reveals low standard deviation values, which demonstrates the production of NDX particles with consistent size and zeta potential batch to batch.

NDX Drug Loading Analysis

A standard curve (**Figure 2**) was generated by measuring the absorbance of samples with known concentrations of Dox in 2.5 mM NaOH, since NDX was synthesized in the same conditions. Based on the absorbance values of the supernatant from the NDX synthesis process, the concentration of Dox in the supernatant was determined. Although there is a concern that Dox has low solubility in a basic environment in an aqueous solution, the maximum concentration of Dox in the standard curve dilutions was 50 μg/ml. Additionally, with high drug loading efficiency, the concentration of Dox in the supernatant after NDX synthesis was no more than ~30 μg/ml. These concentrations are well below the solubility parameter of 10 mg/ml for Dox-HCl in water. The total amount of Dox in the supernatant was subtracted from the amount of Dox added to determine the amount of Dox loaded into the nanodiamond complexes. Loading

efficiency was obtained by dividing the amount of Dox loaded by the amount of Dox added initially for synthesis. Drug loading analysis demonstrated high loading efficiency across all 10 batches of NDX (**Table 2**). The loading efficiency ranged from 84.0% to 90.7%, with an average of 87.8%, proving nanodiamonds to be a very effective carrier of Dox. Loading was also very consistent across the batches, with a resulting standard deviation of 2.2%.

NDX Drug Release Analysis

Standard curves (**Figures 3 and 4**) were generated by plotting fluorescence intensity versus concentration of Dox in two sets of media—a 1:1 ratio and a 1:10 ratio of 10% FBS in DMEM to PBS. The amount of Dox released at every time point was determined based on the concentration of Dox and the volume of the supernatant. The release of Dox was analyzed over a period of ten days with fluorescence measurements taken for the first five hours and then every 24 hours until finish. Drug release analysis demonstrates a sustained release of Dox from NDX. Refer to **Figure 5** for the drug release profiles for all 10 batches plotted as percentage of Dox released over time. **Table 3** summarizes the percentage of Dox released at specific points (5 hours, 1 day, 5 days, and 10 days) as well as the average and standard deviation values in the two different sets of media. The amount of Dox released in the 1:1 medium after 10 days (64%) is almost 20% points higher than that of the 1:10 medium (45.1%). This direct correlation between percentage of Dox released and concentration of FBS in the media suggests that FBS contributes to the release of Dox from NDX. The proposed mechanism is that the proteins in FBS displace the Dox on the surface of the nanodiamonds at a faster rate than PBS does. Although 100% drug release was not obtained, the drug release experiments in this study were performed for only 240 hours.

However, a previous study by Chow et al. was performed for 400 hours, which resulted in 100% drug release. Therefore, if the experiments were performed for a longer period, 100% release would be achieved. Yet for the purposes of this study, only a 240 experiment period was necessary since nanodiamonds are cleared from the body within that time frame. Statistical analysis of Dox released from NDX demonstrates consistency in the drug release profiles across all 10 batches. The Dox release in the 1:10 media has very low standard deviation values (~1.5), whereas in the 1:1 media, the standard deviation values are slightly higher (~3.0).

NDXLP Size and Zeta Potential Measurements and Distributions

Zetasizer measurements were performed to determine the average size and zeta potential of a batch of NDX prior to synthesis of NDXLP. The resulting NDXLP particles were also measured for their average size and zeta potential as well. **Table 4** summarizes these measurements. The NDX used had an average diameter of 98.9 ± 2.1 nm while the NDXLPs had an average diameter of 161.7 ± 1.4 nm after filtration with a 0.2 μm polycarbonate membrane. The liposomes prepared without NDX have an average diameter of 86.5 ± 1.2 nm. The NDXLPs have a significantly larger size. Considering the size of the NDX complexes and liposomes, the size of NDXLPs also suggests successful incorporation of the NDX with the liposomes. The average zeta potential of the NDXLPs is -1.8 ± 0.8 mV. Incorporation with liposomes also resulted in particles with near neutral surface charge. The distributions of the size and zeta potential measurements were also recorded for analysis. In particular, the zeta potential distribution (**Figure 7**) suggests successful incoporation of NDX with liposomes since there is a

very narrow distribution. The NDX used for synthesis has a surface potential of +43.7 mV, but there is no peak in the distribution around that value.

NDXLP Fluorescent Measurements

Spectral scan for fluorescence of NDX shows a peak wavelength around 590-600 nm (**Figure 8**). Spectral scan of the synthesized NDXLP with DID dye included shows two peaks—one at around 590 nm and the other at around 670 nm (**Figure 9**). The peak at 670 nm represents the DID fluorescent label which is soluble within the lipid bilayer of the particles. The peak at 590 nm represents NDX. This spectral scan is further evidence that suggests the successful incorporation of NDX complexes within the NDXLP particles.

NDXLP Size Exclusion Chromatography Analysis

Size exclusion chromatography (SEC) was performed to separate NDXLPs into different fractions. Refer to **Figure 11** for the fluorescence analysis of the fractions. Every fraction contains the fluorescent signal of both the NDX and the liposomes. The differing ratios of NDX and DID fluorescence across the fractions suggest that there are two subpopulations of NDXLPs—NDX encapsulated by liposomes and NDX-lipid clusters. These results are consistent with the results obtained by Moore et al. in their synthesis and SEC analysis of nanodiamond loaded liposomes.[9] The initial fractions (1-4) contain NDX encapsulated by liposomes because of higher ratios of DID fluorescence signal. This makes sense since the DID fluorescence would be more prominent because the dye is soluble within the hydrophobic region of the lipid bilayer

and is displayed on the exterior of the NDXLPs while the NDX signal is reduced because the complexes are encapsulated within the liposomes. The later fractions (5-12) contain NDX-lipid clusters because of the higher ratio of NDX fluorescence signal as the NDX are clustered around liposomes. Nonetheless, these results demonstrate a strong association between NDX and lipids, which is essential for effective penetration across the mucus barrier.

NDXLP Thermo-stability Study

The NDXLPs were incubated in PBS at 37°C for 4 hours with size measurements taken every hour. The study was conducted for 4 hours since the mucus in the colon is overturned within that time frame. (Lai Adv Drug Del 2009, Brownlee 2003, Lehr 1991, Ensign 2012) **Figure 12** summarizes the results of this study. The initial average size of the particles was 161.70 d.nm. For hours 1, 2, 3, and 4, the average size of the particles were 157.67 d. nm, 164.40 d. nm, 162.17 d. nm, and 157.70 d. nm, respectively. The differences in the size of the particles for every hour can be attributed to random error in the DLS readings. These results suggest that NDXLPs exhibit good size stability in PBS at physiological temperature. The particles would not aggregate within the time frame of mucus turnover. Therefore, this effect would not hinder the NDXLPs from diffusing through the mucus layer.

NDXLP Zeta Potential vs pH

The pH range of the colon can vary from 5.7 to 7.5.[33–35] Therefore, measuring the zeta potential of the NDXLPs across this pH range is important. The results are summarized in **Figure 13**. The

zeta potential of the particles does not vary by much across this pH range, with the differences likely resulting from random error in the zeta potential readings. The particles retain a slight negative charge across this pH range. Consequently, there should be no concerns of the NDXLPs interacting with negatively charged mucins due to electrostatic attraction. Thus, the particles would avoid adhering to the mucins and becoming trapped in the mucus barrier.

NDXLP Mucus Penetration

The composition of human mucus is 95% water and 1.0 to 5% mucin.[26] Polyester membranes were coated with mucus layers composed of 2% wt and 5% wt mucin. The thickness of the mucus layers in the Transwell inserts were adjusted to 150 μm, since the average thickness of mucus in the colon is approximately 100-150 μm.[30,36,37] Since the turnover rate of mucus in the colon is 4-6 hours[37], the NDXLPs were allowed a maximum of 4 hours to diffuse through the mucus barrier. Solution from the bottom compartments were extracted and analyzed for the fluorescence signal of liposomes after 2 and 4 hours. The fluorescence measurements were converted to concentration via a standard curve obtained by serial dilution of NDXLPs with DID label from a specified concentration (**Figure 15**). The total amount of NDXLPs that successfully diffused through the mucus barriers and the membrane were calculated based on the concentration and volume of the solution in the bottom compartment. The total amount of NDXLP that penetrated the mucus layers were compared against the total amount in the control group (no mucus layer) at 2 hours and 4 hours. **Table 5** summarizes the results from the mucus penetration experiment. 89.4% of the particles that were able to diffuse through the permeable membrane were also able to diffuse through 2% mucin after 2 hours. The percentage of particles

that passed through 2% mucin after 4 hours increased slightly to 91.1%. This result makes sense since the bottom and top compartments were approaching equilibrium in terms of NDXLP concentration. With 5% mucin, the percentage penetration was 50.9% after 2 hours and 63.3% after 4 hours. There was a much greater increase in the case of 5% mucin due to a stronger driving force for equilibrium. These results demonstrate that a vast majority of the particles were able to diffuse through 2% mucin. Still, a significant amount of NDXLPs were able to diffuse through the more strongly concentrated 5% mucin. These results demonstrate that NDXLPs indeed have the ability to penetrate the mucus barrier in the colon.

Discussion

A comprehensive study on the physical characteristics of nanodiamond-doxorobucin (NDX) was performed in order to assess the consistency of the NDX synthesis method. NDX size, surface potential, drug loading, and drug release were characterized across 10 individual batches. The standard deviation values across the batches for every parameter were low. Furthermore, the standard deviation values for are comparable to other drug delivery systems such as PEGylated liposomal doxorubicin (Doxil, Caelyx) and nab-paclitaxel (Abraxane). For example, drug loading efficiency for PEGylated liposomal doxorubicin is 96.3 ± 2.2%.[38] For nab-paclitaxel, mean particle size is 130-150 nm[39] and drug loading ranges from 89-98%.[40] Doxil and Abraxane are FDA approved nano-scale drug delivery systems for the treatment of cancer. On the other hand, NDX size is 116.7 ± 6.4 nm and drug loading efficiency is 87.8 ± 2.2%. Comparisons to FDA approved treatments help gauge the allowed deviation that the FDA desires in its assessment of new investigational drug platforms. Additionally, according to a FDA guidance document for in vitro/ in vivo correlations of extended release oral dosage forms: "the maximum recommended range at any dissolution time point specification should be ± 10% of label claim deviation from the mean dissolution profile obtained from the clinical/bioavailability lots."[41] The deviation values for drug release in the NDX model are certainly well below the allowed deviation of ± 10% at any given time point (**Table 3**). This is by no means a direct validation of NDX, since the guidance document refers to an in vitro/in vivo correlation for an oral dosage form. However, the guidance document sets a guideline for deviation that in which the NDX drug release results can be compared to. Thus far, the NDX model for drug release is consistent and within the FDA limits. Overall, this characterization study is part of the translational work required to further push the NDX platform towards clinical testing. The results

from this study suggest that the method of synthesis for NDX produces particles with consistent physical properties.

After characterization of NDX, the other focus of this thesis was to modify NDX for the purposes of localized treatment of colon cancer. The characteristics of NDX that prevented its effectiveness for this specific application included severe aggregation of the complexes in high ionic environments as well as their highly positive surface charge (+50mV), causing strong adhesion to mucins. The high zeta potential is likely due to the presence of protonated Dox molecules clustered on the surface of the complexes.[11] Therefore, incorporation of NDX with liposomal carriers was necessary to produce particles that could remain stable and penetrate the mucus barrier in the colon. Rehydration of a lipid thin film with a concentrated NDX solution produced self-assembled NDX-loaded liposomes (NDXLPs). There are a number of features of NDXLPs that contribute to its potential success as a drug delivery system. First of all the size of the NDXLPs allow them to diffuse relatively quickly through the mucin mesh network of the mucus barrier. The spacing of the mucus mesh has been reported be between 200 nm[37] and 1 μm.[42] The NDXLPs have an average size of ~160 nm, suggesting that the particles can fit through the mucus mesh. Additionally, another study showed that particles with sizes smaller than 200 nm still had significant translocation permeability in mucus.[43] Furthermore, NDXLPs do not aggregate in PBS at physiological temperature. The thermo-stability of these particles prevents them from becoming too big, such that that they no longer fit through the pores of the mucin mesh. The charge of the NDXLPs is also essential for their ability to penetrate the mucus. Electrostatic attraction between a positively-charged nanoparticle surface and the extensive negatively charged sugar moieties on mucins are strongly mucoadhesive.[44] In addition, nanoparticles with anionic cores exhibiting surface charges more negative than -10 mV

experienced significant mucoadhesion.[32] However, PEGylated particles with surface charges between -2 mV and -6 mV penetrated mucus at rates not much lower than those in pure water.[32] A particle with a net neutral surface charge would be ideal to avoid any type of electrostatic attraction and thus adhesion to mucins. NDXLPs exhibit an average zeta potential of ~ -2 mV. The incorporation of a zwitterionic lipid bilayer with NDX likely counteracts the highly positive surface charge of the NDX complexes, which explains the significantly decreased zeta potential. The NDXLP surface charge is still net negative but very close to neutral, suggesting a very small amount of electrostatic interaction. Unmodified liposomes tend to be good mucoadhesive delivery systems as well due to the significant amounts of lipids present in the mucus.[44,45] The incorporation of nonionic long chain polymers such as PEG or Pluronic onto the surface of liposomal carriers greatly improves their permeability through the mucus layer. One study demonstrated an 85% increase in diffusion efficiency for liposomes incorporated with Pluronic F-127 versus unmodified liposomes.[27] Besides improving the transport of liposomal carriers across mucus, Pluronic can also enhance their stability. High ionic content and the presence of bile salts can severely compromise liposomal carriers. However, a previous study demonstrated negligible aggregation of Pluronic F-127 incorporated liposomes in simulated gastric fluid and minor aggregation in simulated intestinal fluid.[28] Since NDXLPs combine all of the aforementioned features: fairly small size, near neutral surface charge, and surface functionalization with long chain polymers, their success in penetrating the mucus layers (2% and 5% wt mucin), as demonstrated by this study, was expected.

Two different subpopulations of NDXLPs— NDX encapsulated liposomes and NDX-liposome clusters—were synthesized based on the results of size exclusion chromatography fraction analysis. The fluorescence analysis for the fractions is consistent with the fluorescence

analysis performed by Moore et al. on their nanodiamond-epirubicin loaded liposomes, which also existed in two similar subpopulations.[9] Additionally, they demonstrated this by CryoTEM imaging.[9] Moore et al. also showed successful incorporation of nanodiamond complexes into liposomes using confocal microscopy and flow cytometry analysis based on the fluorescence signals from DID and AlexaFluor488 covalently attached to the surface of the nanodiamonds.[9] The method of synthesis used by Moore et al. involved rehydration of a lipid thin film with a solution of nanodiamond-drug complex as well. The nanodiamond-drug complexes encapsulated within liposomes have been shown to be about twice as large versus the nanodiamond-drug-liposome clusters[9], which explains the broad size distribution. Yet, this dual population of NDXLPs still exhibited a narrow distribution for surface charge. The thermo-stability study in PBS at physiological temperature also demonstrated that both subpopulations have size stability. The main difference between the varying subpopulations of NDXLPs is their inherent sizes, with the NDX-liposome clusters likely having faster diffusion across the mucus barrier as a result.

Future Work

For future studies, NDXLPs can be tested in an in vitro model with a mucus-secreting colorectal cancer cell line, such as Caco2, for cell uptake and cell viability as described in previous studies.[27,29] For cell uptake studies, the NDXLPs will be placed in media and allowed to incubate with the cancer cells for 2 hours and 4 hours. Then, the media is aspirated and discarded and the cells are rinsed with buffer. Fluorescence analysis will be performed to measure the DID signal to determine the amount of NDXLPs that were able to penetrate the mucus barrier and become endocytosed by the cells. For cell viability studies, the NDXLPs will not contain the fluorescent DID label. The cells will be treated with NDXLPs for 2 and 4 hours. Afterwards, media is discarded and cells are rinsed. The cells are then cultured for an additional 3 days. A cell viability assay (MTT assay) will be conducted after the 3-day incubation to assess the apoptotic effect of the NDXLPs.

Furthermore, NDXLPs can be studied in vivo using a rodent model. The animals will be treated to be induce colorectral cancer as described in previous studies.[46] The NDXLPs will be administered weekly through barium enema in a degradable gel. The mice are then analyzed for NDXLP localization by whole body imaging for the fluorescence signature of DID. Biodistribution analysis will be performed by fluorescence imaging analysis of specific organs[11] every other day for a week after initial administration. Serum analysis to measure myelosuppression as well as biomarkers for kidney and liver damage will be performed to assess NDXLP toxicity in vivo.[9,11] Finally, the mice will be sacrificed after 8 weeks and the tumor extracted and measured for weight. NDXLP performance in terms of toxicity and tumor mass will be compared to a negative control (PBS) and a positive control (NDX). Based on the results of previous studies and the studies from this thesis, NDXLPs can be expected to have enhanced

drug efficacy and improved drug tolerance in addition to increased tumor uptake and localization for colorectal cancer models.

The properties of NDXLPs also make them applicable for oral administration in treatment of cancer. The advantages of oral administration include convenience and high patient compliance. However, there are significant barriers to oral administration of drugs, such as the harsh environment within the gastrointestinal tract, protective mucus layers, and first-pass metabolism. Drugs administered orally first arrive in the stomach, where the gastric environment is highly acidic for the purpose of digestion. After the stomach, drugs enter the small intestine. Drugs are absorbed through the enterocytes in the small intestine into the hepatic portal system. These drugs then pass through the liver where they are metabolized by hepatic enzymes before entering systemic circulation. NDXLPs have not been tested for their stability in gastric conditions. However, an enteric coating can be used to protect these nanoparticles until they arrive in the small intestine, where the pH is much less extreme—6.0 to 7.4 in humans.[33] The studies provided in this work have demonstrated that NDXLPs maintain a slight negative charge across a pH range of 5.5 to 7.5. Furthermore, previous studies have demonstrated the stability of Pluronic incorporated liposomes in simulated intestinal fluid.[28] NDXLPs have also demonstrated mucus penetration properties. The thickness of the mucus barrier coating the epithelium of the small intestine (~20 μm) is significantly smaller than that of the colon (~150 μm).[30] Thus, NDXLPs can be expected to maintain stability in the small intestine and effectively penetrate its mucus barrier. Once the NDXLPs are absorbed into the epithelium and the enterocytes, they are then transported to the liver for metabolism. The incorporation of long polymer chains on the surface such as PEG or Pluronic has been shown to increase resistance to enzyme degradation.[47] Also, a previous study demonstrated successful oral delivery of human epidermal growth factor

with PEGylated liposomes.[48] After passing through the liver, NDXLPs now enter systemic circulation. These particles can passively target tumor tissues by accumulating in their leaky vasculature in what is known as the EPR effect. The NDXLPs have an average size ~160 nm, which is significantly below the threshold of 400 nm required to take advantage of the EPR effect.[49] Also, the PEG chains on the surface of the NDXLPs help to reduce rapid clearance by the reticuloendothelial system, thus increasing circulation time.[9] Additionally, NDXLPs can be functionalized for targeted delivery by attaching antibodies or ligands to the ends of the polymer chains. Targeted delivery with nanodiamond-liposomes have been shown to induce tumor regression in a previous study by Moore et al. as drug uptake was further increased in cancer cells expressing the target molecule.[9] However, the addition of a targeting agent may affect the mucus penetration ability of the particles which would hinder their use in oral administration. Overall, the physical characteristics of NDXLPs make them a potential drug delivery system for cancer treatment through oral administration.

NDXLPs are one specific form of nanodiamond-liposome particle developed for the specific purpose of delivering doxorubicin to cancer cells across a mucus barrier. But, the nanodiamond-liposome platform can be readily adapted for a multitude of different applications. Moore et al. developed a nanodiamond-epirubin-loaded liposome system functionalized with anti-EGFR antibodies for the targeted delivery of epirubicin. Nanodiamonds have already been proven to be effective carriers for therapeutics such as anthracyclines and siRNA.[9–11,25] They were also shown to improve the safety and efficacy of imaging agents such as Gd(III).[50] Additionally, nanodiamond-liposome particles can be outfitted with a broad range of targeting agents, such as antibodies or ligands. These targeting agents are usually attached to one end of modified PEG chains on the surfaces of PEGylated liposomal carriers. This being the case,

nanodiamond-liposomes could be functionalized with a specific targeting agent to treat a particular disease, such as anti-CD20 antibody for treatment of lymphoma. Furthermore, they could be applied as agents in cancer imaging. The flexibility of this system along with its effect on increasing the efficacy and safety of therapeutics and imaging agents make nanodimaond-liposomes a promising drug delivery platform with potential clinical translation.

Tables and Figures

Figure 1: Diagram of NDX synthesis. A) ND and free Dox, B) ND and Dox modication after addition of NaOH, C) NDX complex formation

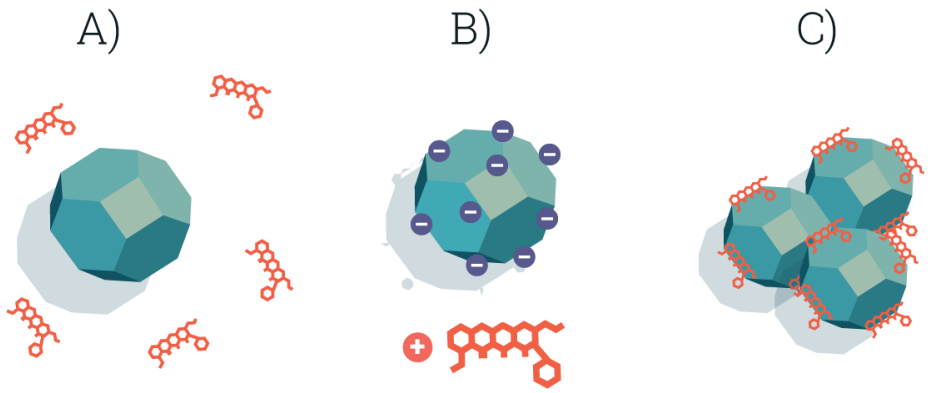

Table 1: NDX Size and Zeta Potential Measurements

Batch	Z-average Size	PDI	Zeta Potential
1	119.4	0.20	49.8
2	115.6	0.17	46.5
3	116.6	0.18	45.7
4	124.8	0.18	53.5
5	124.5	0.16	49.5
6	111.0	0.15	53.4
7	123.6	0.21	51.9
8	106.1	0.16	53.8
9	114.3	0.15	46.8
10	110.7	0.20	52.3
Overall Average	116.7	0.18	50.3
Overall Std Dev	6.4	0.02	3.1

Figure 2: Standard curve plot for concentration of Dox vs Absorbance

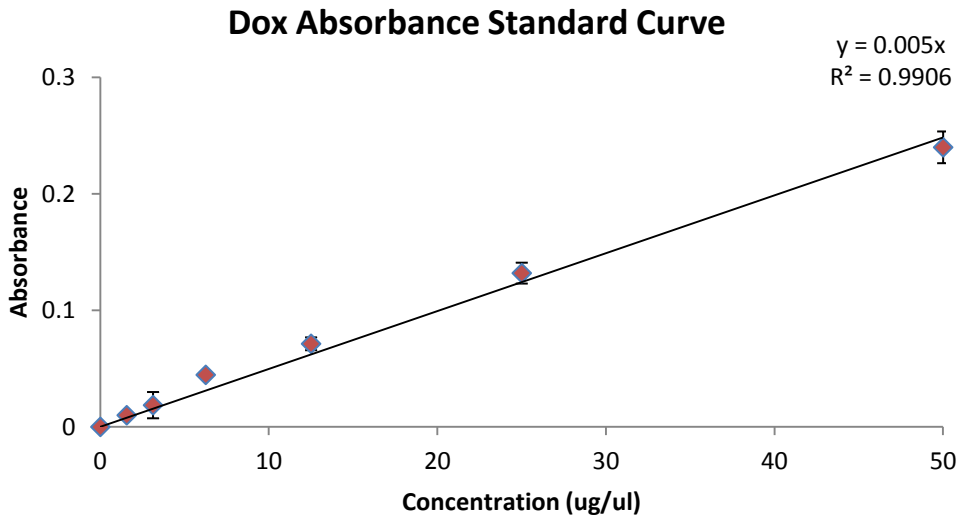

Table 2: NDX drug loading efficiency for doxorubicin

Batch	Drug Loading Efficiency
1	87.5%
2	88.1%
3	87.9%
4	86.6%
5	84.8%
6	90.5%
7	90.7%
8	89.4%
9	88.2%
10	84.0%
Average	87.8%
Std Dev	2.2%

Figure 3: Standard curve for concentration of Dox vs Fluorescence Intensity in 1:1 Media

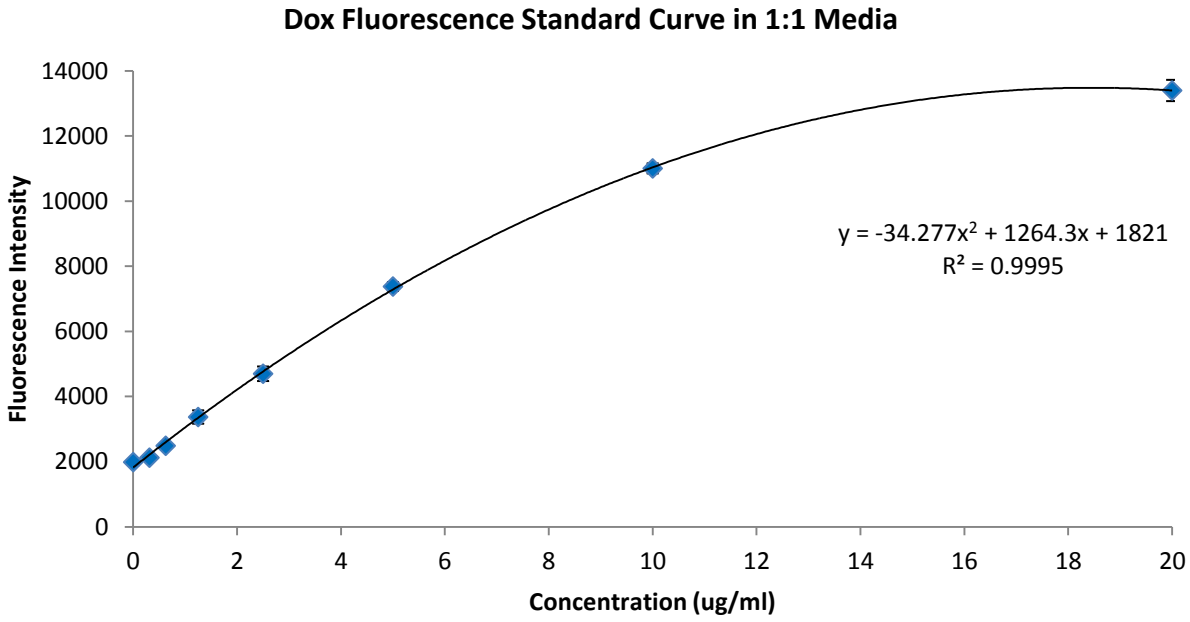

Figure 4: Standard curve for concentration of Dox vs Fluorescence Intensity in 1:10 Media

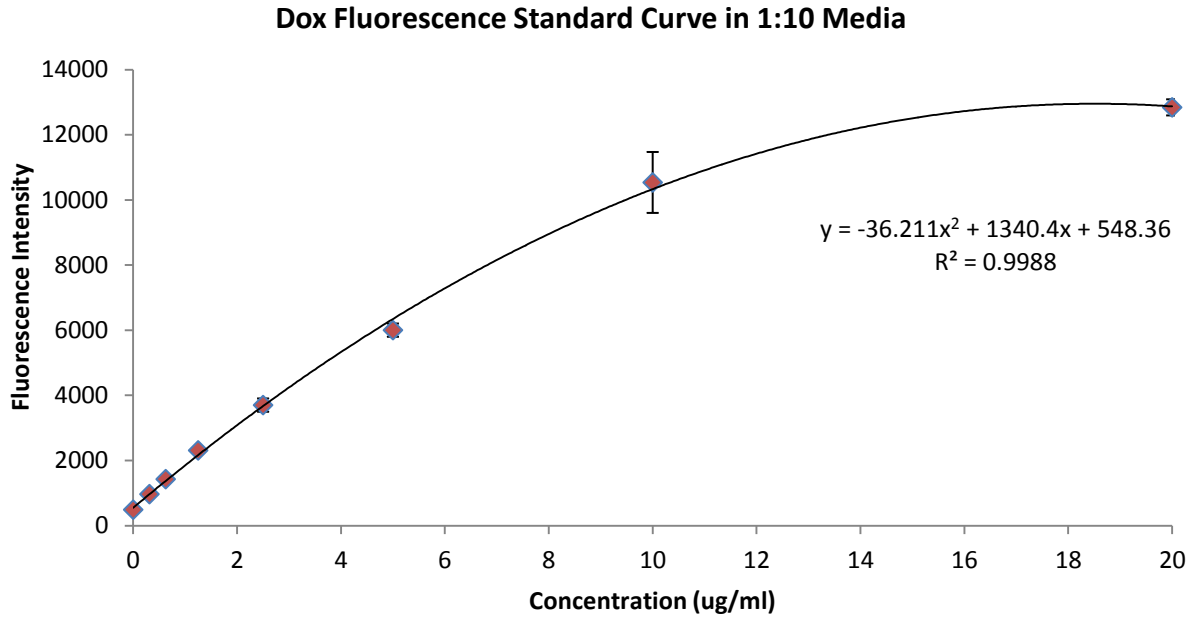

Figure 5: NDX Drug Release Profiles for Batches 1 through 10

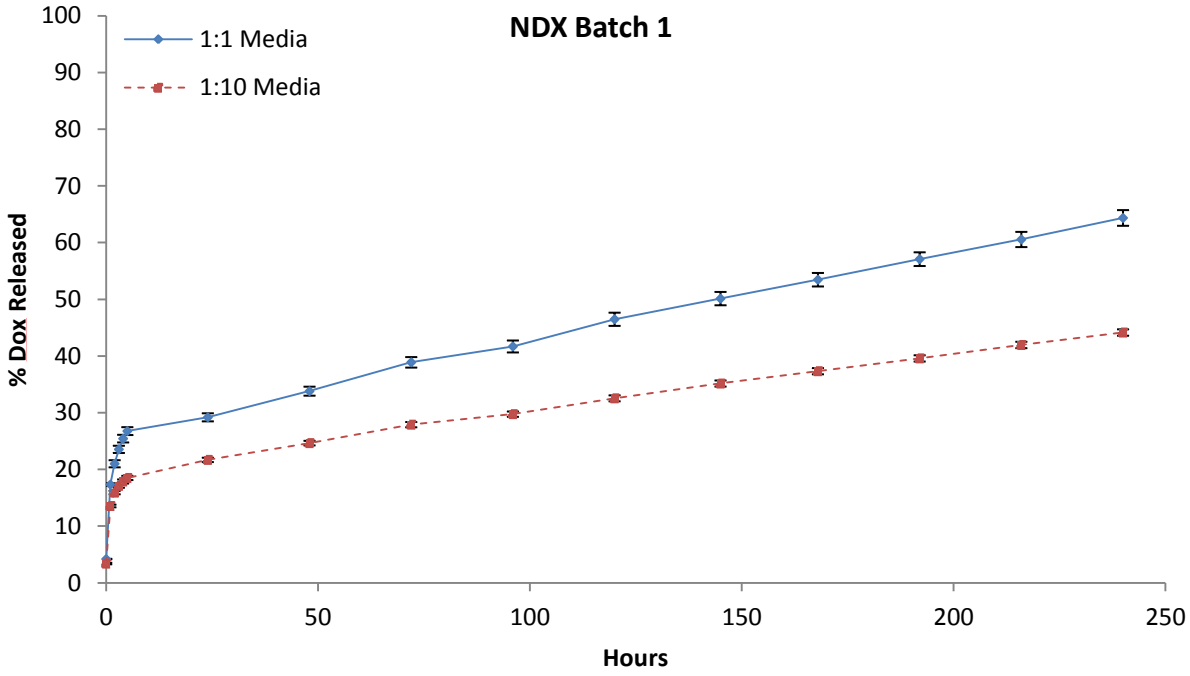

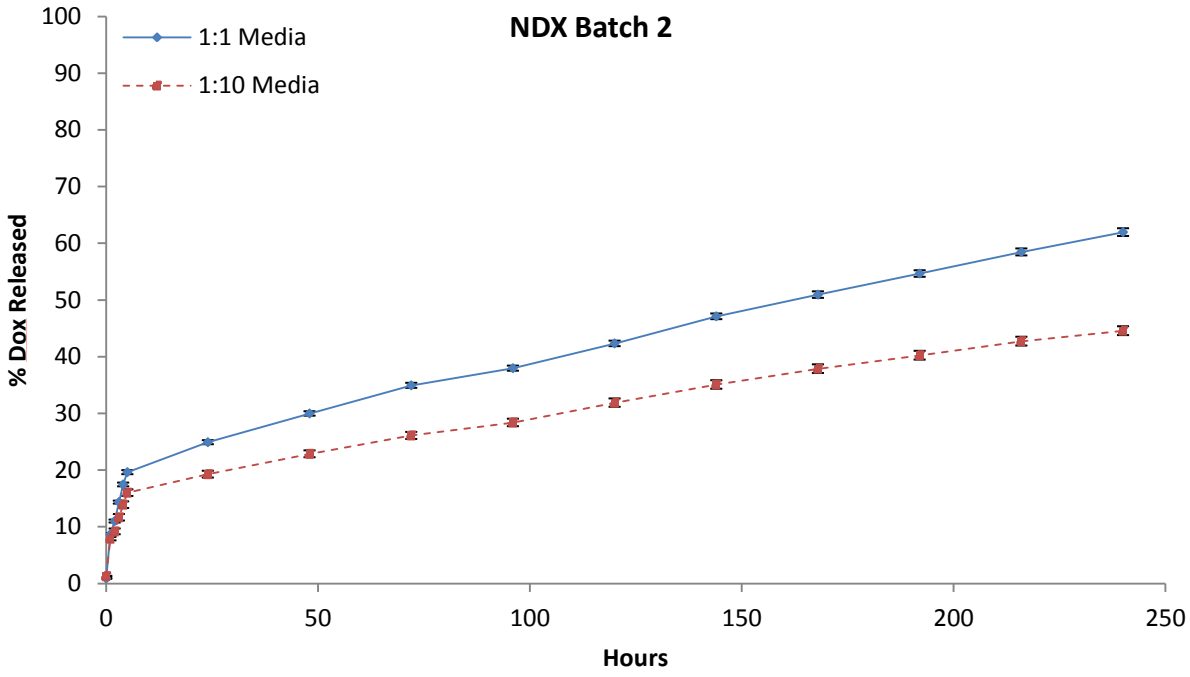

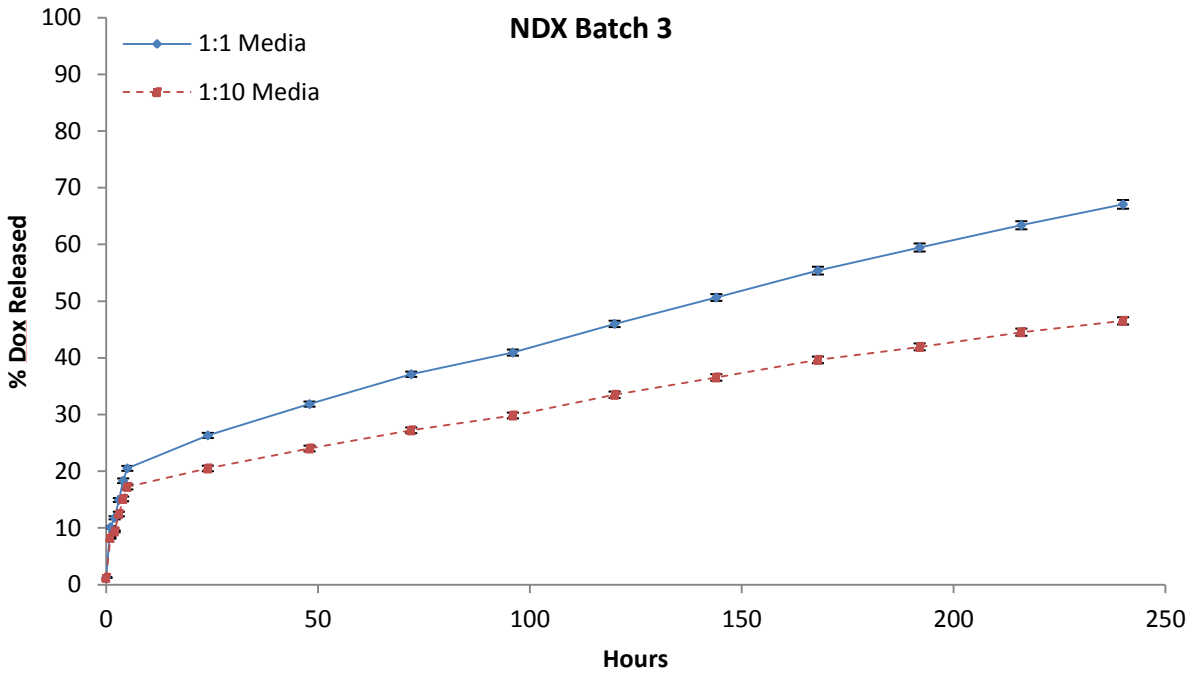
NDX Batch 3
1:1 Media
1:10 Media
% Dox Released
Hours
0
10
20
30
40
50
60
70
80
90
100
0
50
100
150
200
250

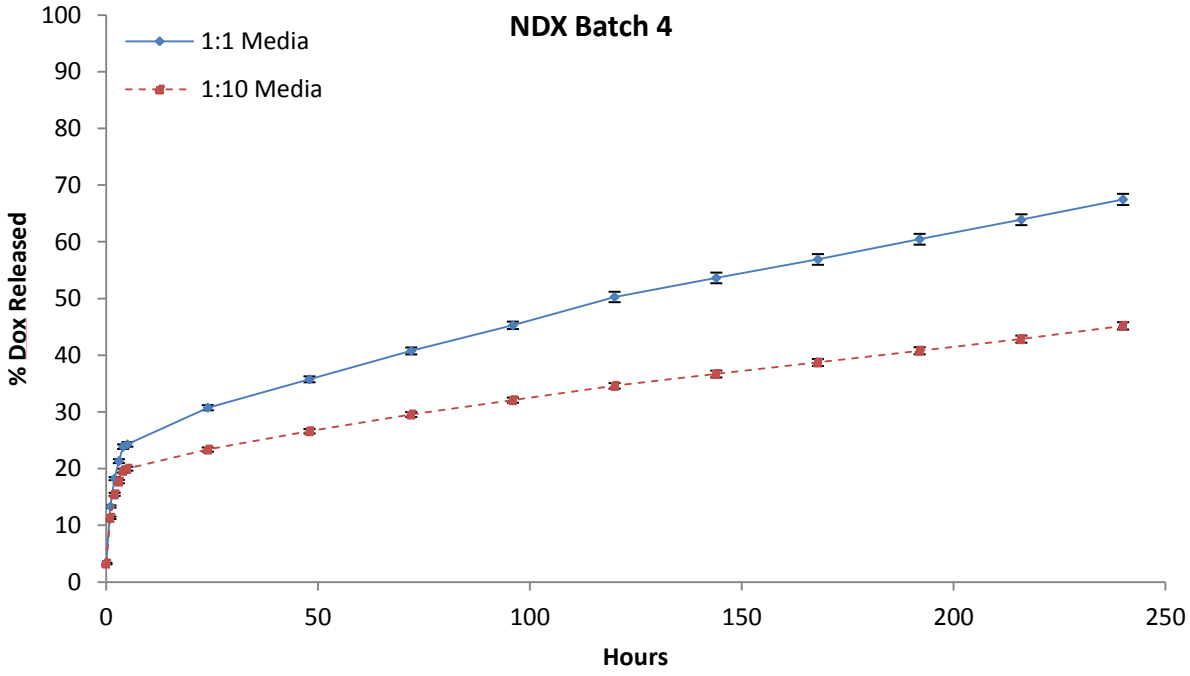
NDX Batch 4
1:1 Media
1:10 Media
% Dox Released
Hours
0
10
20
30
40
50
60
70
80
90
100
0
50
100
150
200
250

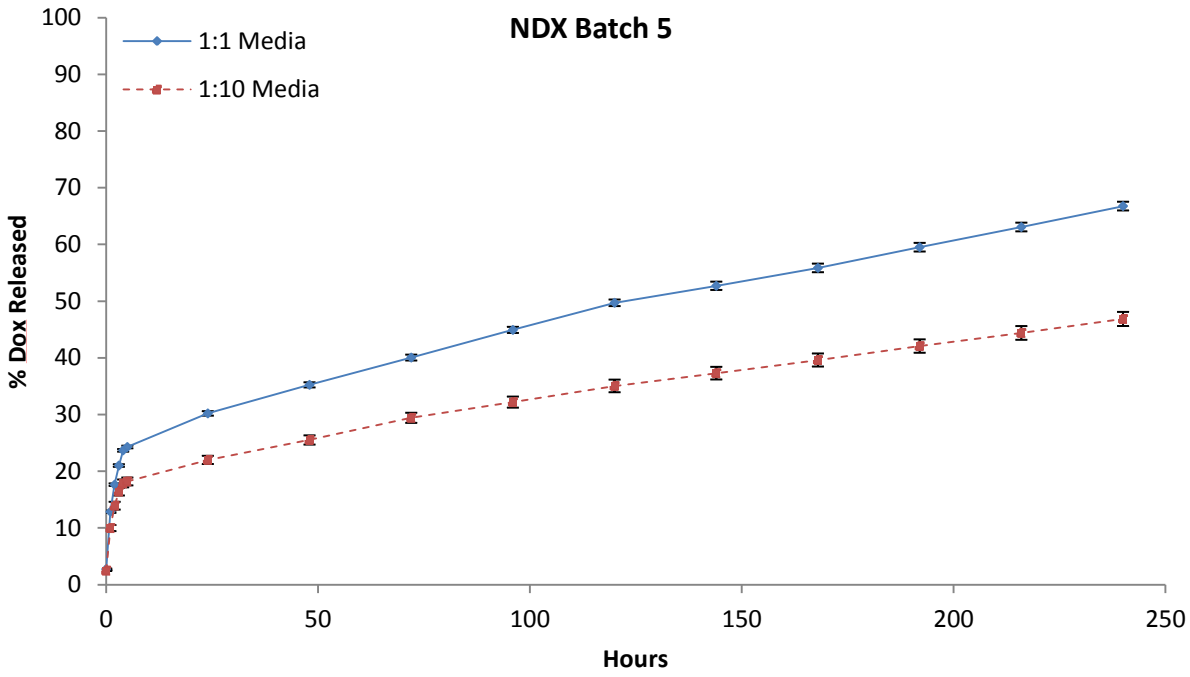
NDX Batch 5
1:1 Media
1:10 Media
% Dox Released
Hours
0
10
20
30
40
50
60
70
80
90
100
0
50
100
150
200
250

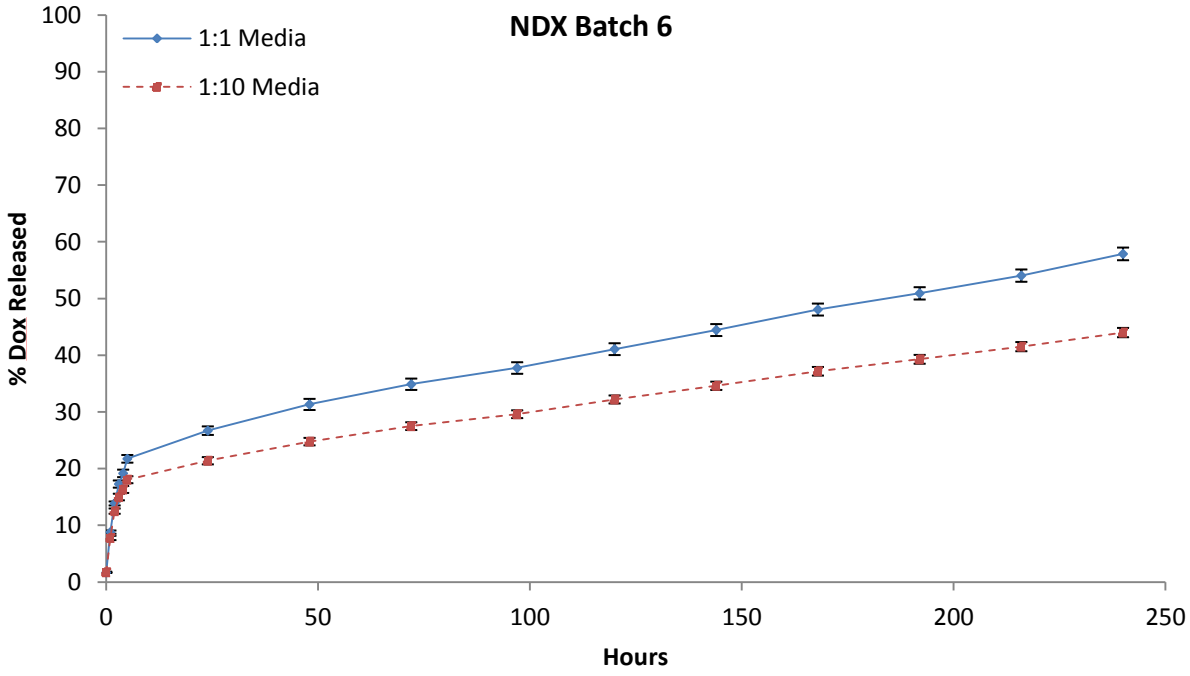
NDX Batch 6
1:1 Media
1:10 Media
% Dox Released
Hours
0
10
20
30
40
50
60
70
80
90
100
0
50
100
150
200
250

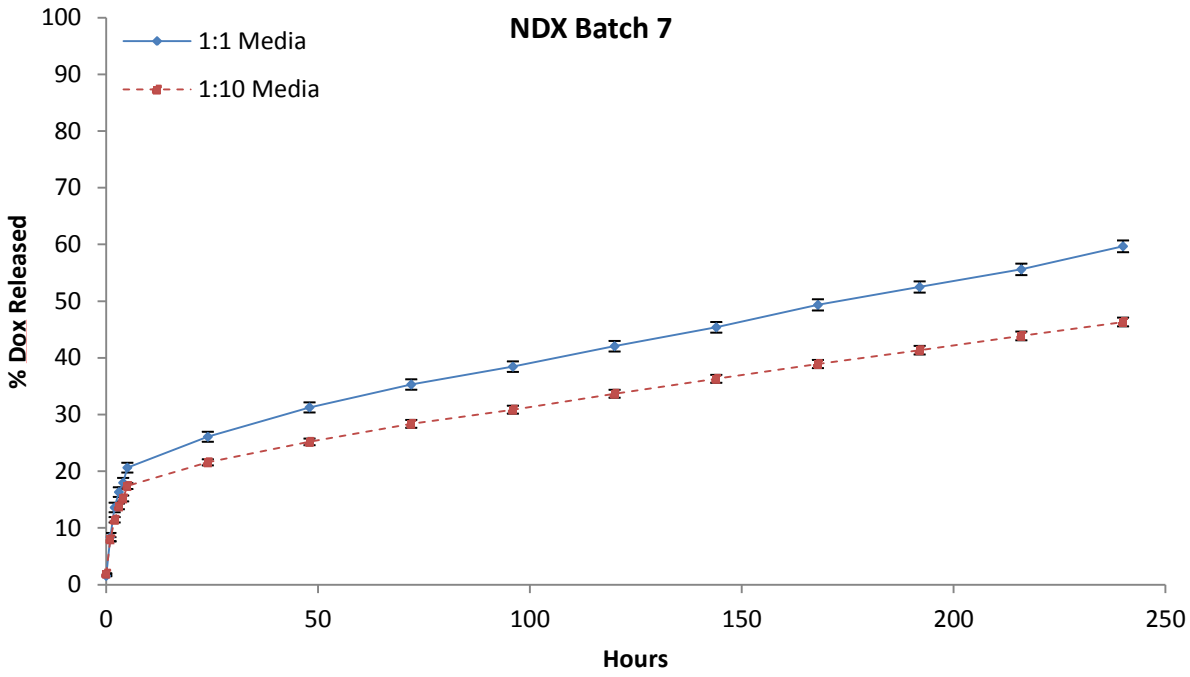
NDX Batch 7
1:1 Media
1:10 Media
% Dox Released
Hours
0
10
20
30
40
50
60
70
80
90
100
0
50
100
150
200
250

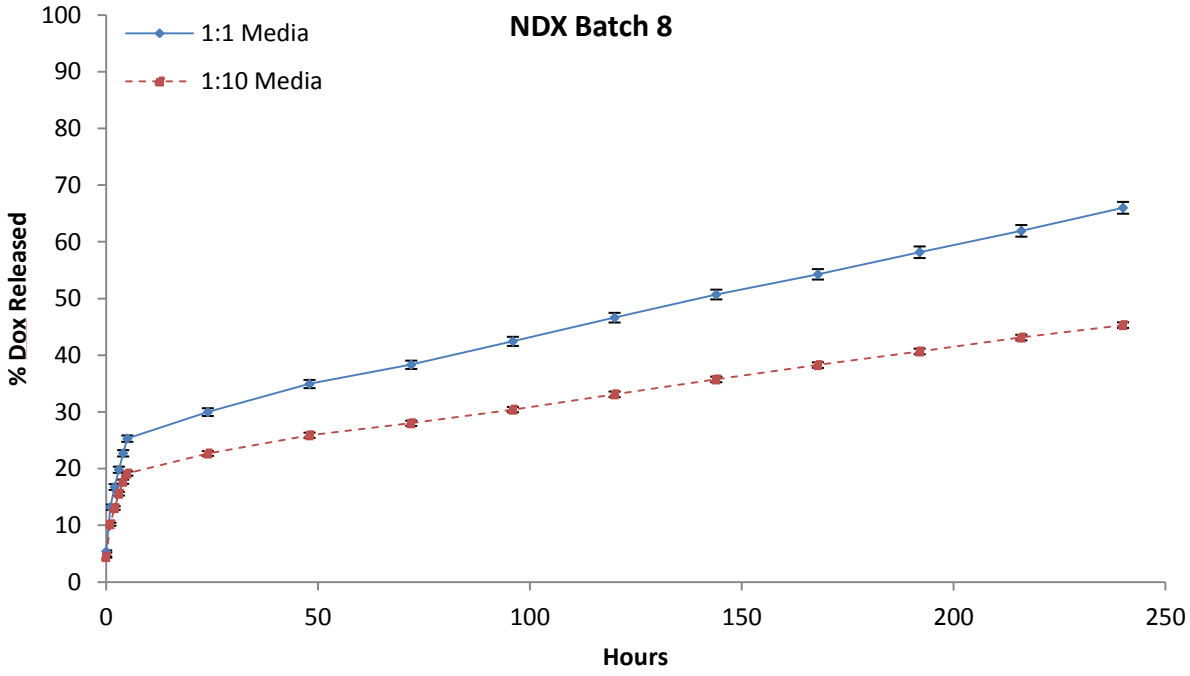
NDX Batch 8
1:1 Media
1:10 Media
% Dox Released
Hours
0
10
20
30
40
50
60
70
80
90
100
0
50
100
150
200
250

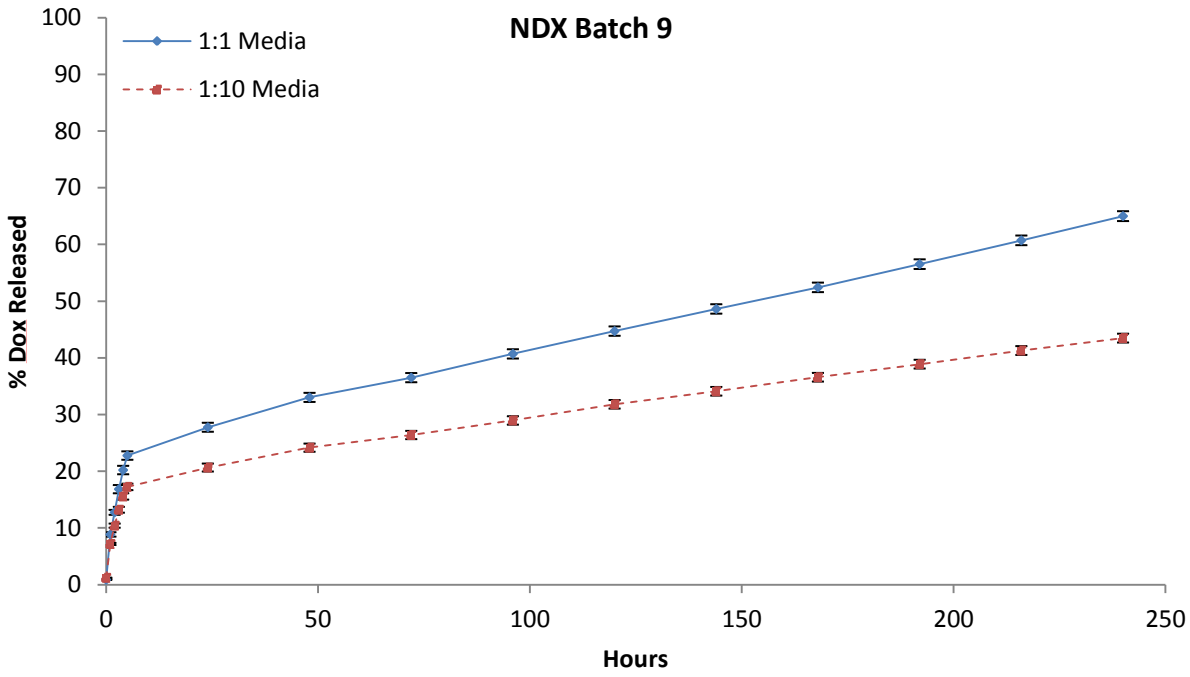
NDX Batch 9
1:1 Media
1:10 Media
% Dox Released
Hours
0
10
20
30
40
50
60
70
80
90
100
0
50
100
150
200
250

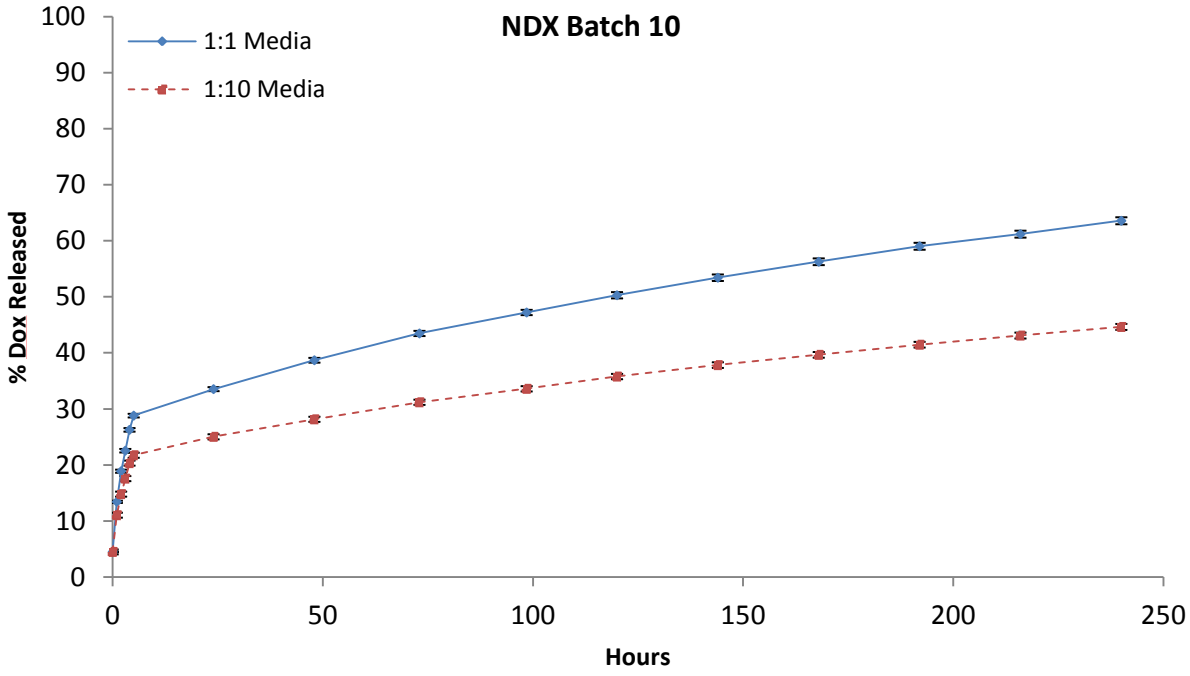
NDX Batch 10
1:1 Media
1:10 Media
% Dox Released
Hours
0
10
20
30
40
50
60
70
80
90
100
0
50
100
150
200
250

Table 3: Cumulative amount of Dox released at specific time points throughout incubation

1:1 Media to PBS					1:10 Media to PBS				
Batch	Hr 5	Day 1	Day 5	Day 10	Batch	Hr 5	Day 1	Day 5	Day 10
1	26.8	29.2	46.5	64.4	1	18.5	21.7	32.6	44.2
2	19.6	24.9	42.3	62.0	2	16.0	19.3	31.9	44.6
3	20.5	26.3	46.0	67.1	3	17.2	20.5	33.5	46.5
4	24.3	30.8	50.3	67.5	4	20.0	23.4	34.6	45.2
5	24.3	30.2	49.7	66.8	5	18.2	22.0	35.0	46.9
6	21.7	26.7	41.1	57.9	6	18.1	21.4	32.2	44.0
7	20.6	26.1	42.0	59.7	7	17.4	21.6	33.7	46.3
8	25.3	30.0	46.6	66.0	8	19.2	22.7	33.1	45.3
9	22.8	27.8	44.7	65.0	9	17.2	20.7	31.8	43.5
10	28.8	33.5	50.3	63.6	10	21.7	25.0	35.8	44.6
Average	23.5	28.5	46.0	64.0	Average	18.4	21.8	33.4	45.1
Std Dev	3.0	2.7	3.4	3.2	Std Dev	1.6	1.6	1.4	1.1

Figure 6: Schematic of NDXLP Synthesis

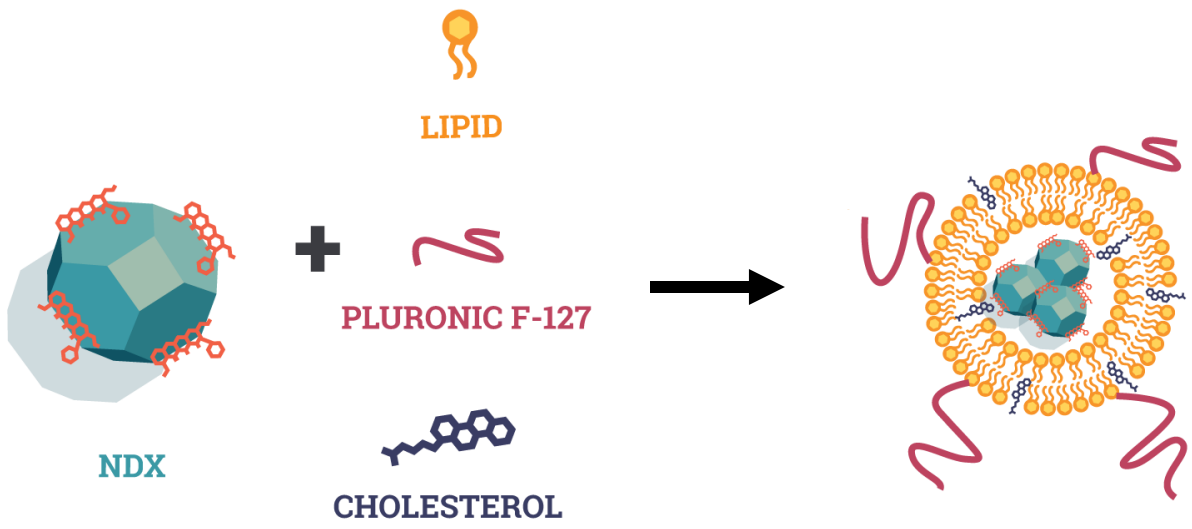

Figure 7: Size and zeta potential distribution analysis for NDXLP

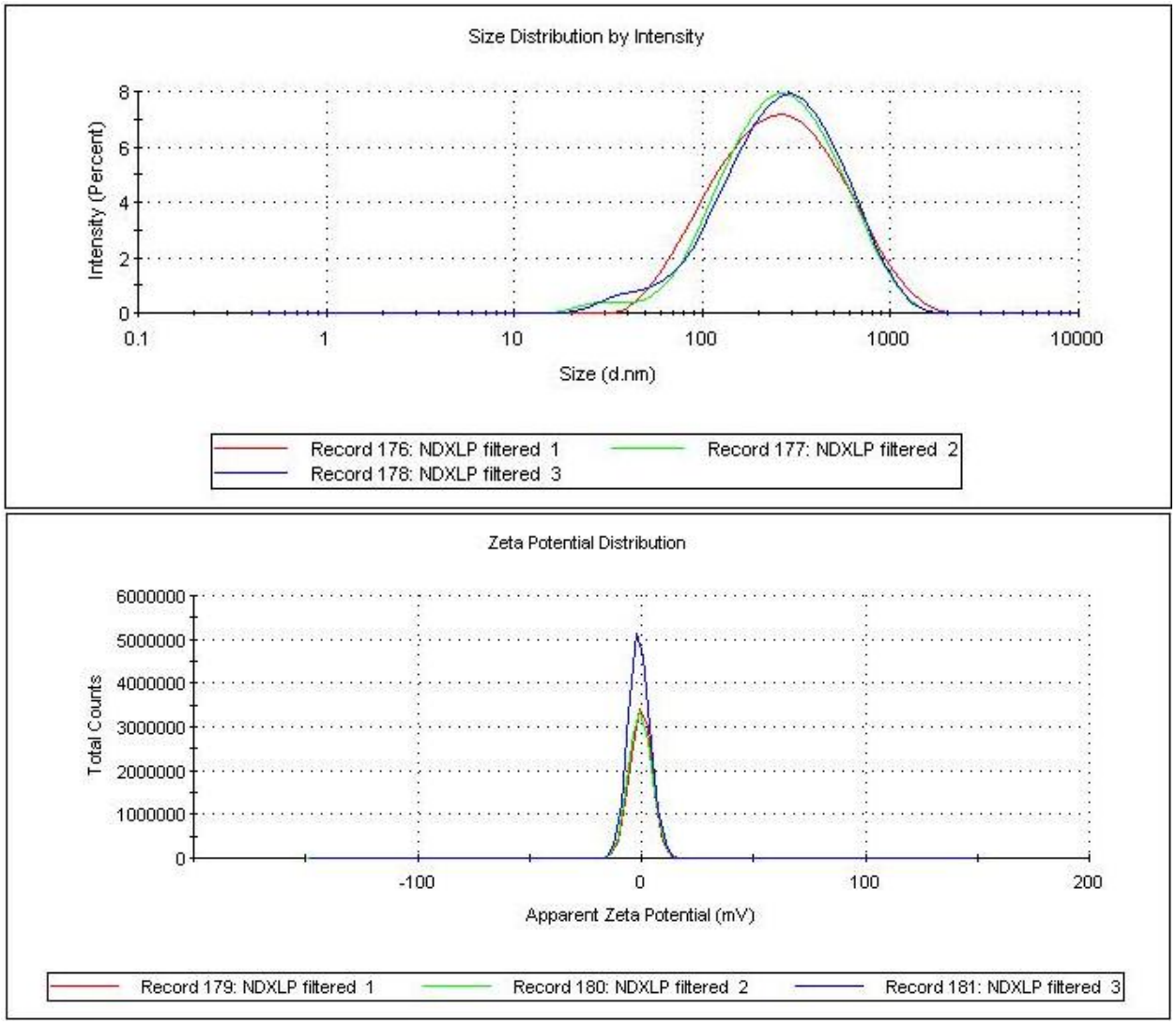

Table 4: NDX, Liposome, and NDXLP size and zeta potential. NDXLP was synthesized from this particular batch of NDX.

	NDX	Liposome	NDXLP
Size (d.nm)	98.9 ± 2.1	86.5 ± 1.2	161.7 ± 1.4
Zeta Potential (mV)	+43.7 ± 1.9	-6.0 ± 1.3	-1.8 ± 0.8

Figure 8: Fluorescent analysis of NDX

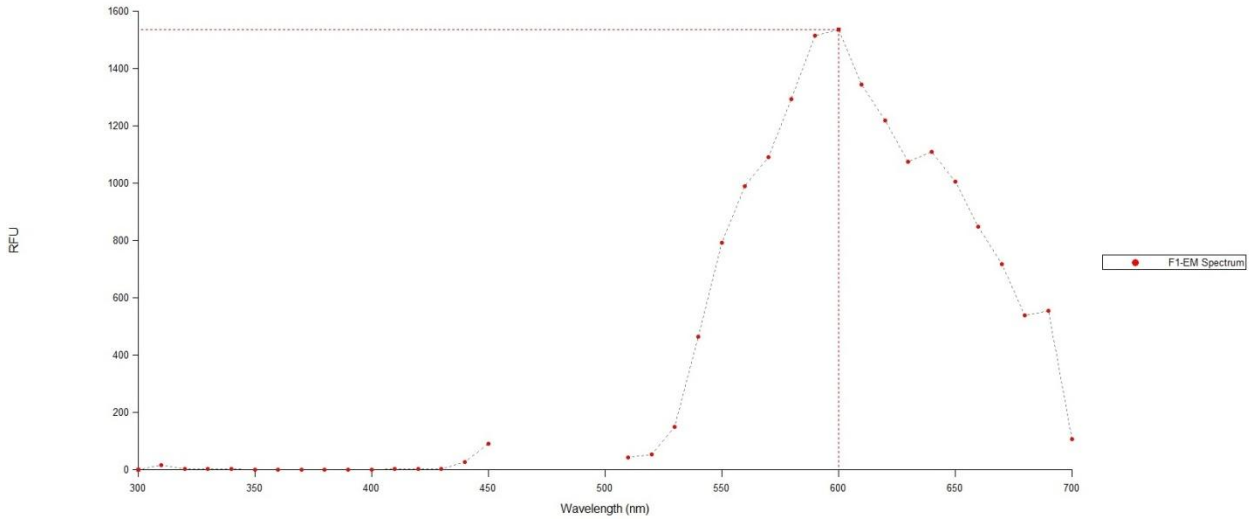

Figure 9: Fluorescent analysis of NDXLP with DID fluorescent dye

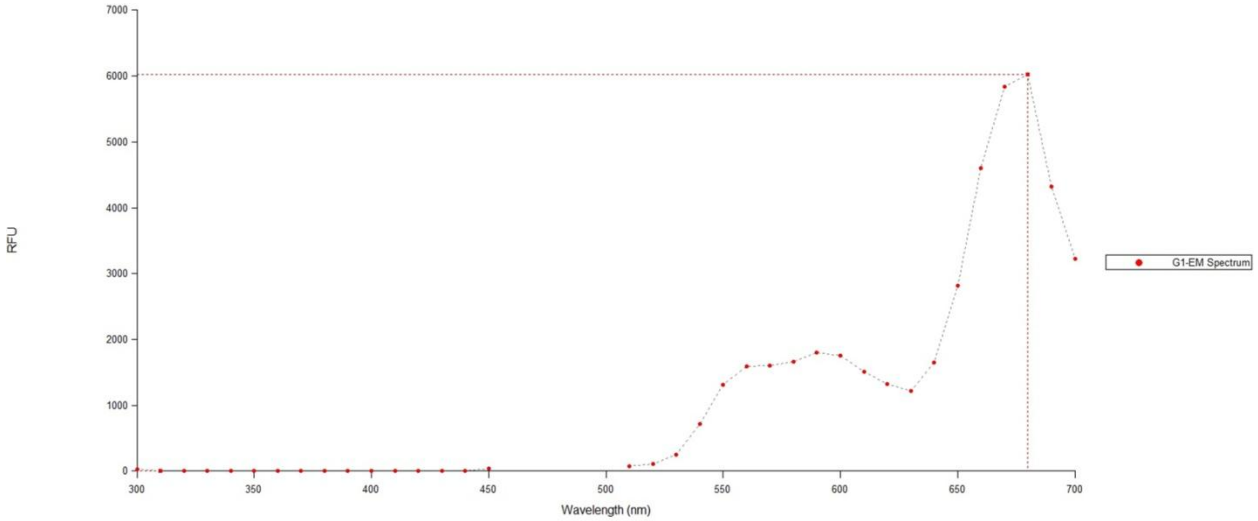

Figure 10: NDXLP and NDX diluted to 0.5 mg/ml (in terms of ND) in PBS

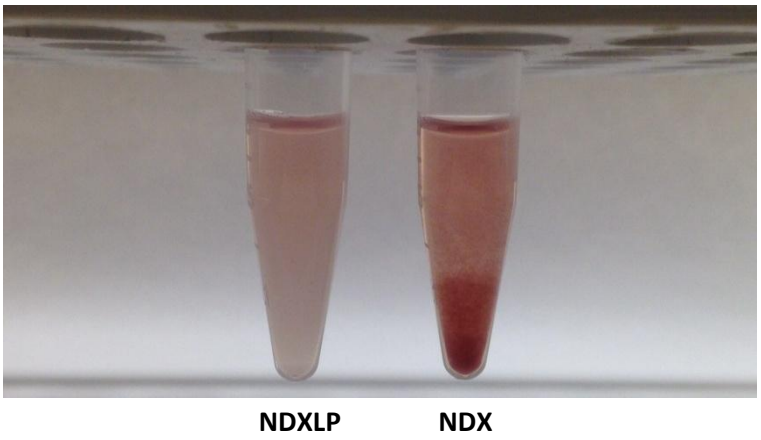

Figure 11: Fluorescent analysis of NDXLP fractions separated by size-exclusion chromatography

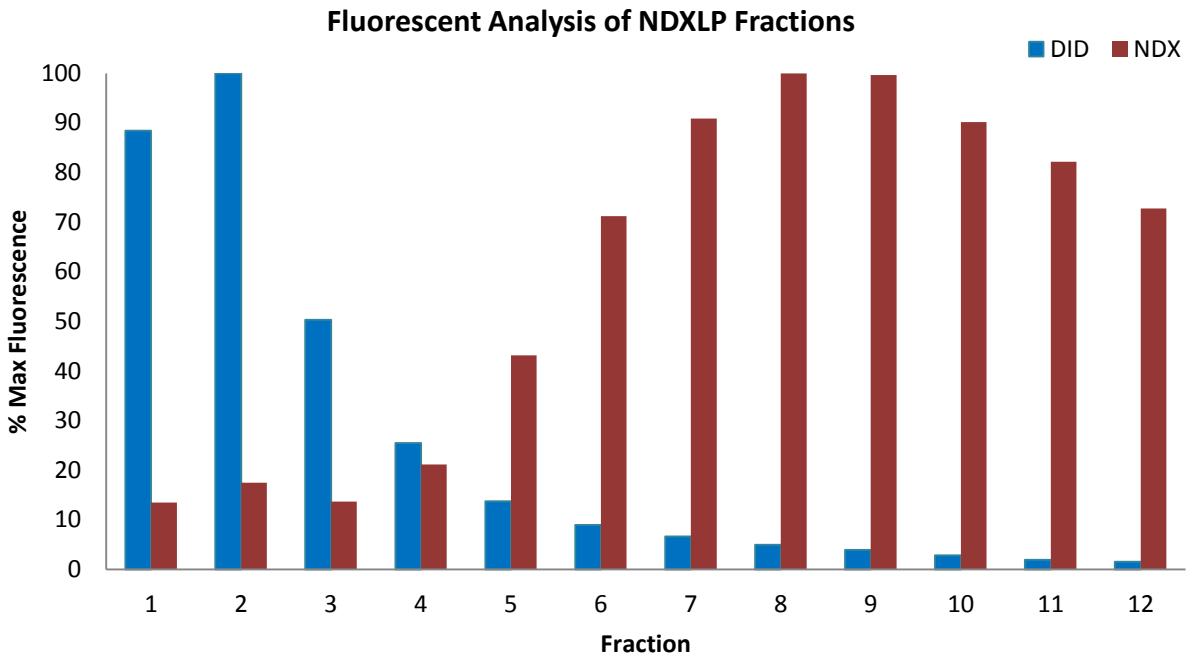

Figure 12: NDXLP Thermo-stability in PBS at 37°C

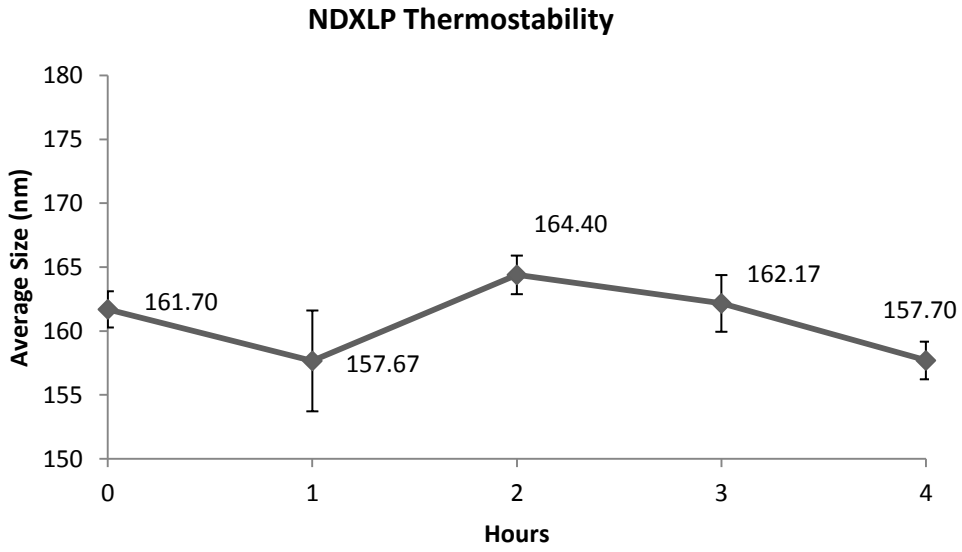

Figure 13: NDXLP zeta potential across colon pH range

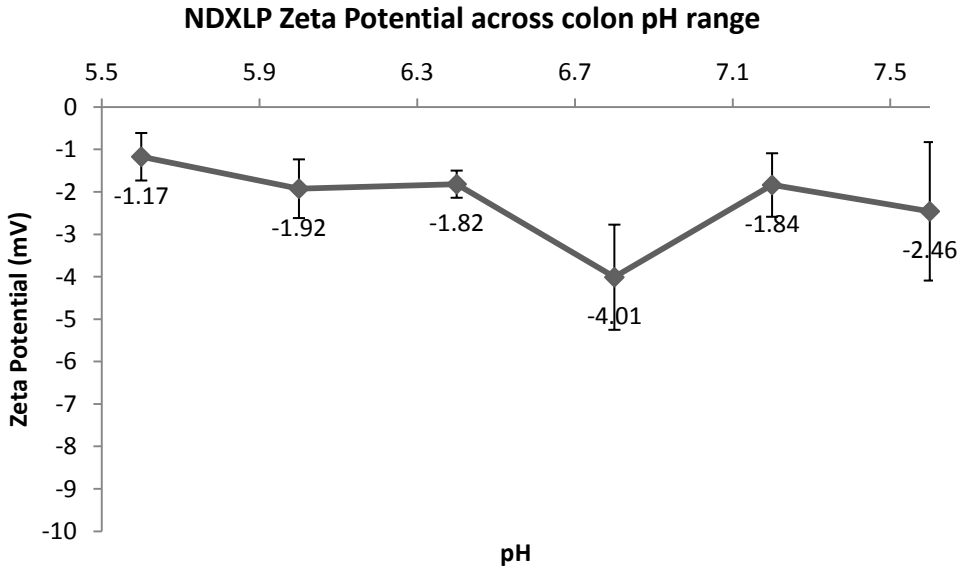

Figure 14: Schematic of mucus penetration experiment

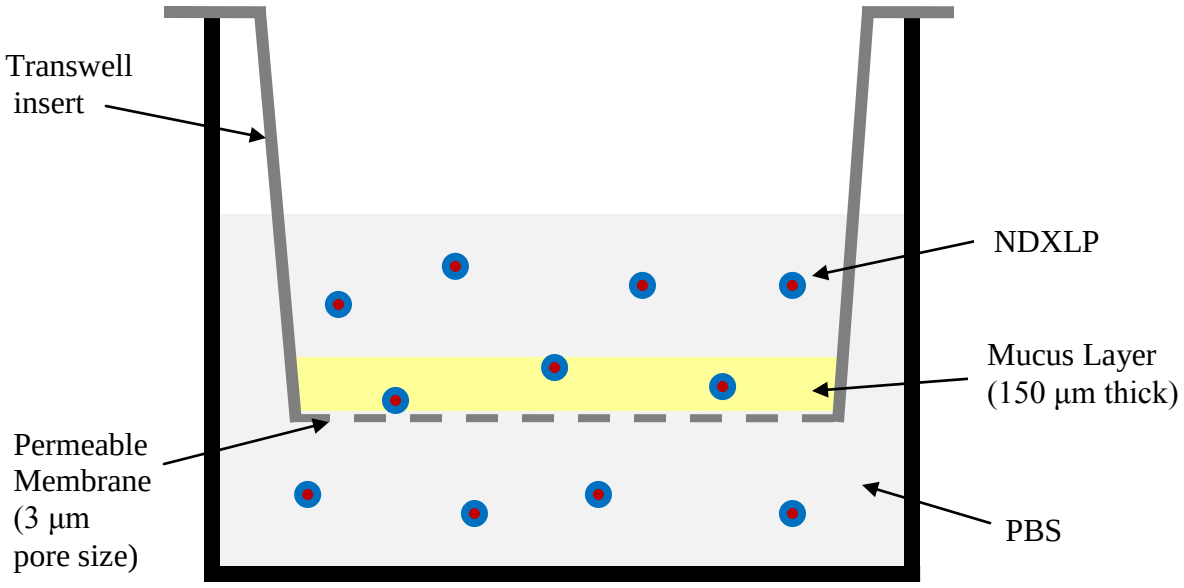

Figure 15: Standard curve for concentration of Lipid (mg/mL) vs DID fluorescence

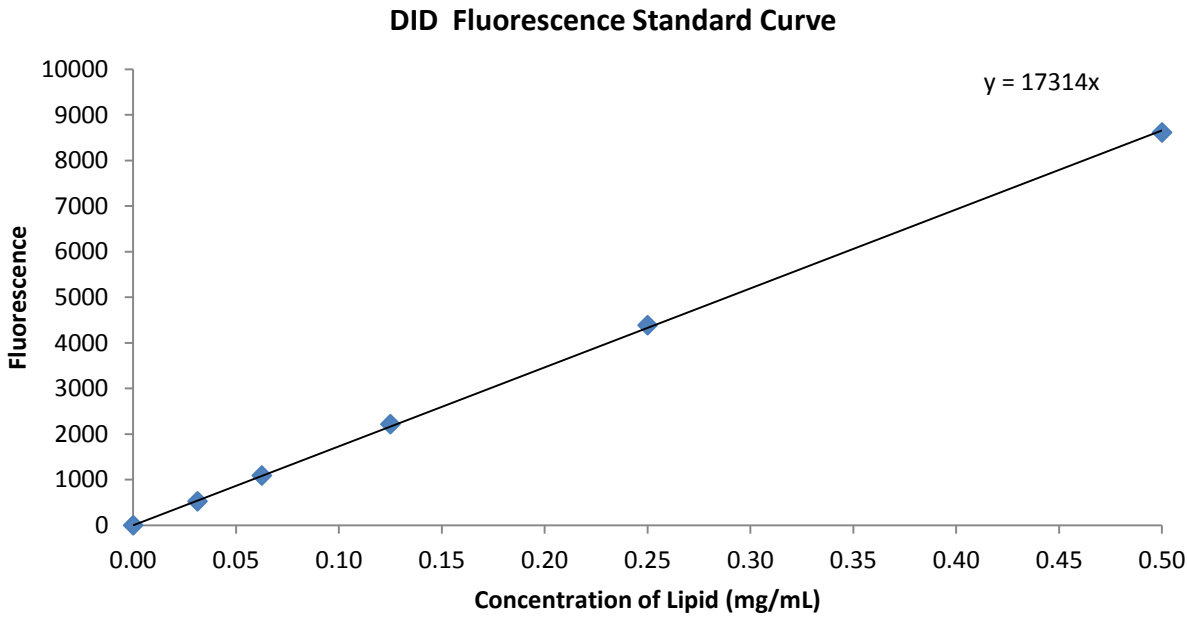

Table 5: NDXLP mucus penetration experiment summary. Percentage of the control (membrane only) that passed through the respective mucus layers after two and four hours.

Coating	2 hr	4 hr
2% Mucin	89.4%	91.1%
5% Mucin	50.9%	63.3%

References

1. Colorectal Cancer. *Am. Cancer Soc.* (2014). at <http://www.cancer.org/cancer/colonandrectumcancer/detailedguide/colorectal-cancer-key-statistics>

2. Chang, G. J. Challenge of primary tumor management in patients with stage IV colorectal cancer. *J. Clin. Oncol.* **30,** 3165–6 (2012).

3. Hellinger, M. D. & Santiago, C. A. Reoperation for recurrent colorectal cancer. *Clin. Colon Rectal Surg.* **19,** 228–36 (2006).

4. Weiser, M. R. *et al.* Individualized prediction of colon cancer recurrence using a nomogram. *J. Clin. Oncol.* **26,** 380–5 (2008).

5. Longley, D. B. & Johnston, P. G. Molecular mechanisms of drug resistance. *J. Pathol.* **205,** 275–92 (2005).

6. Gottesman, M. M., Fojo, T. & Bates, S. E. Multidrug resistance in cancer: role of ATP-dependent transporters. *Nat. Rev. Cancer* **2,** 48–58 (2002).

7. Goldstein, L. J. *et al.* Expression of a multidrug resistance gene in human cancers. *J. Natl. Cancer Inst.* **81,** 116–24 (1989).

8. Fojo, A. T. *et al.* Expression of a multidrug-resistance gene in human tumors and tissues. *Proc. Natl. Acad. Sci. U. S. A.* **84,** 265–9 (1987).

9. Moore, L., Chow, E. K.-H., Osawa, E., Bishop, J. M. & Ho, D. Diamond-lipid hybrids enhance chemotherapeutic tolerance and mediate tumor regression. *Adv. Mater.* **25,** 3532–41 (2013).

10. Xi, G. *et al.* Convection-enhanced delivery of nanodiamond drug delivery platforms for intracranial tumor treatment. *Nanomedicine* **10,** 381–91 (2014).

11. Chow, E. K. *et al.* Nanodiamond therapeutic delivery agents mediate enhanced chemoresistant tumor treatment. *Sci. Transl. Med.* **3,** 73ra21 (2011).

12. Tacar, O., Sriamornsak, P. & Dass, C. R. Doxorubicin: an update on anticancer molecular action, toxicity and novel drug delivery systems. *J. Pharm. Pharmacol.* **65,** 157–70 (2013).

13. Cancer multidrug resistance. *Nat. Biotechnol.* 94–95 (1999).

14. Dönmez, Y., Akhmetova, L., İşeri, Ö. D., Kars, M. D. & Gündüz, U. Effect of MDR modulators verapamil and promethazine on gene expression levels of MDR1 and MRP1 in doxorubicin-resistant MCF-7 cells. *Cancer Chemother. Pharmacol.* **67,** 823–8 (2011).

15. Argov, M., Kashi, R., Peer, D. & Margalit, R. Treatment of resistant human colon cancer xenografts by a fluoxetine-doxorubicin combination enhances therapeutic responses comparable to an aggressive bevacizumab regimen. *Cancer Lett.* **274,** 118–25 (2009).

16. Ramachandran, C., Rabi, T., Fonseca, H. B., Melnick, S. J. & Escalon, E. A. Novel plant triterpenoid drug amooranin overcomes multidrug resistance in human leukemia and colon carcinoma cell lines. *Int. J. Cancer* **105,** 784–9 (2003).

17. Rabindran, S. K. *et al.* Reversal of a Novel Multidrug Resistance Mechanism in Human Colon Carcinoma Cells by Fumitremorgin C. 5850–5859 (1998).

18. Weinländer, G. *et al.* Treatment of advanced colorectal cancer with doxorubicin combined with two potential multidrug-resistance-reversing agents: high-dose oral tamoxifen and dexverapamil. *J. Cancer Res. Clin. Oncol.* **123,** 452–5 (1997).

19. Kornblau, S. M. *et al.* Phase I study of mitoxantrone plus etoposide with multidrug blockade by SDZ PSC-833 in relapsed or refractory acute myelogenous leukemia. *J. Clin. Oncol.* **15,** 1796–802 (1997).

20. Mross, K. *et al.* Randomized phase II study of single-agent epirubicin +/- verapamil in patients with advanced metastatic breast cancer. An AIO clinical trial. Arbeitsgemeinschaft Internistische Onkologie of the German Cancer Society. *Ann. Oncol.* **4,** 45–50 (1993).

21. Mochalin, V. N., Shenderova, O., Ho, D. & Gogotsi, Y. The properties and applications of nanodiamonds. *Nat. Nanotechnol.* **7,** 11–23 (2012).

22. Huang, H., Pierstorff, E., Osawa, E. & Ho, D. Active Nanodiamond Hydrogels for Chemotherapeutic Delivery. (2007).

23. Huang, L.-C. L. & Chang, H.-C. Adsorption and Immobilization of Cytochrome c on Nanodiamonds. *Langmuir* **20,** 5879–5884 (2004).

24. Zhang, X.-Q. *et al.* Polymer-functionalized nanodiamond platforms as vehicles for gene delivery. *ACS Nano* **3,** 2609–16 (2009).

25. Chen, M. *et al.* Nanodiamond Vectors Functionalized with Polyethylenimine for siRNA Delivery. *J. Phys. Chem. Lett.* **1,** 3167–3171 (2010).

26. Lieleg, O., Vladescu, I. & Ribbeck, K. Characterization of particle translocation through mucin hydrogels. *Biophys. J.* **98,** 1782–9 (2010).

27. Li, X. *et al.* Novel mucus-penetrating liposomes as a potential oral drug delivery system: preparation, in vitro characterization, and enhanced cellular uptake. *Int. J. Nanomedicine* **6,** 3151–62 (2011).

28. Chen, D. *et al.* Comparative study of Pluronic(®) F127-modified liposomes and chitosan-modified liposomes for mucus penetration and oral absorption of cyclosporine A in rats. *Int. J. Pharm.* **449,** 1–9 (2013).

29. Zhu, Q. *et al.* Pluronic F127-modified liposome-containing tacrolimus-cyclodextrin inclusion complexes: improved solubility, cellular uptake and intestinal penetration. *J. Pharm. Pharmacol.* **65,** 1107–17 (2013).

30. Ensign, L. M., Cone, R. & Hanes, J. Oral drug delivery with polymeric nanoparticles: the gastrointestinal mucus barriers. *Adv. Drug Deliv. Rev.* **64,** 557–70 (2012).

31. Lai, S. K. *et al.* Rapid transport of large polymeric nanoparticles in fresh undiluted human mucus. *Proc. Natl. Acad. Sci. U. S. A.* **104,** 1482–7 (2007).

32. Wang, Y.-Y. *et al.* Addressing the PEG mucoadhesivity paradox to engineer nanoparticles that "slip" through the human mucus barrier. *Angew. Chem. Int. Ed. Engl.* **47,** 9726–9 (2008).

33. Fallingborg, J. Intraluminal pH of the human gastrointestinal tract. *Dan. Med. Bull.* **46,** 183–96 (1999).

34. Pye, G., Evans, D. F., Ledingham, S. & Hardcastle, J. D. Gastrointestinal intraluminal pH in normal sub jects and those with colorectal adenoma or carcinoma. 1355–1357 (1990).

35. NUGENT, S. G. Intestinal luminal pH in inflammatory bowel disease: possible determinants and implications for therapy with aminosalicylates and other drugs. *Gut* **48,** 571–577 (2001).

36. Pullan, R. D. *et al.* Thickness of adherent mucus gel on colonic mucosa in humans and its relevance to colitis. *Gut* **35,** 353–9 (1994).

37. Lai, S. K., Wang, Y.-Y. & Hanes, J. Mucus-penetrating nanoparticles for drug and gene delivery to mucosal tissues. *Adv. Drug Deliv. Rev.* **61,** 158–71 (2009).

38. Niu, G., Cogburn, B. & Hughes, J. Preparation and characterization of doxorubicin liposomes. *Methods Mol. Biol.* **624,** 211–9 (2010).

39. Gaitanis, A. & Staal, S. Liposomal doxorubicin and nab-paclitaxel: nanoparticle cancer chemotherapy in current clinical use. *Methods Mol. Biol.* **624,** 385–92 (2010).

40. ABRAXANE® for Injectable Suspension (paclitaxel protein-bound particles for injectable suspension) (albumin-bound) Initial U.S. Approval: 2005. 1–24 (2013).

41. FDA. *Guidance for Industry Guidance for Industry Extended Release Oral Dosage Forms: Development, Evaluation, and Application of In Vitro/In Vivo Correlations*. 18 (1997).

42. Cu, Y. & Saltzman, W. M. Drug delivery: Stealth particles give mucus the slip. *Nat. Mater.* **8,** 11–3 (2009).

43. Norris, D. A. & Sinko, P. J. Effect of size, surface charge, and hydrophobicity on the translocation of polystyrene microspheres through gastrointestinal mucin. *J. Appl. Polym. Sci.* **63,** 1481–1492 (1997).

44. Ensign, L. M., Schneider, C., Suk, J. S., Cone, R. & Hanes, J. Mucus Penetrating Nanoparticles: Biophysical Tool and Method of Drug and Gene Delivery. *Adv. Mater.* **24,** 3887–3894 (2012).

45. Karn, P. R., Vanić, Z., Pepić, I. & Skalko-Basnet, N. Mucoadhesive liposomal delivery systems: the choice of coating material. *Drug Dev. Ind. Pharm.* **37,** 482–8 (2011).

46. Ding, W. *et al.* A novel local anti-colorectal cancer drug delivery system: negative lipidoid nanoparticles with a passive target via a size-dependent pattern. *Nanotechnology* **24,** 375101 (2013).

47. Kim, H., Kim, Y. & Lee, J. Liposomal formulations for enhanced lymphatic drug delivery. *Asian J. Pharm. Sci.* **8,** 96–103 (2013).

48. Li, H., Song, J. H., Park, J. S. & Han, K. Polyethylene glycol-coated liposomes for oral delivery of recombinant human epidermal growth factor. *Int. J. Pharm.* **258,** 11–9 (2003).

49. Yeo, Y. *Nanoparticulate Drug Delivery Systems: Strategies, Technologies, and Applications*. 198 (John Wiley & Sons, 2013). at <https://books.google.com/books?id=iHXMSL_oyvcC&pgis=1>

50. Manus, L. M. *et al.* Gd(III)-nanodiamond conjugates for MRI contrast enhancement. *Nano Lett.* **10,** 484–9 (2010).